THE UNIVERSITY of EDINBURGH

Edinburgh Research Explorer

Resolving small-scale forest snow patterns using an energy-balance snow model with a 1-layer canopy

Citation for published version:
Mazzotti, G, Essery, R, Moeser, CD & Jonas, T 2020, 'Resolving small-scale forest snow patterns using an energy-balance snow model with a 1-layer canopy', *Water Resources Research*, vol. 56, no. 1. https://doi.org/10.1029/2019WR026129

Digital Object Identifier (DOI):
10.1029/2019WR026129

Link:
Link to publication record in Edinburgh Research Explorer

Document Version:
Peer reviewed version

Published In:
Water Resources Research

General rights
Copyright for the publications made accessible via the Edinburgh Research Explorer is retained by the author(s) and / or other copyright owners and it is a condition of accessing these publications that users recognise and abide by the legal requirements associated with these rights.

Take down policy
The University of Edinburgh has made every reasonable effort to ensure that Edinburgh Research Explorer content complies with UK legislation. If you believe that the public display of this file breaches copyright please contact openaccess@ed.ac.uk providing details, and we will remove access to the work immediately and investigate your claim.

OPEN ACCESS

Download date: 27. Jan. 2020

Resolving small-scale forest snow patterns using an energy-balance snow model with a 1-layer canopy

Giulia Mazzotti[1,2]*, Richard Essery[3], C. David Moeser[4], Tobias Jonas[1]

[1] WSL Institute for Snow and Avalanche Research SLF, Davos Dorf, Switzerland

[2] Laboratory of Hydraulics, Hydrology and Glaciology, ETHZ, Zurich, Switzerland

[3] School of Geosciences, University of Edinburgh, Edinburgh, UK

[4] U.S. Geological Survey, New Mexico Water Science Center, Albuquerque, NM, USA

* Correspondence to: G. Mazzotti, giulia.mazzotti@slf.ch

Key points:

- Alternative strategies to represent fine-scale forest canopy structure within a standard energy-balance snow model were tested.
- Only canopy representations that distinguish between near and distant canopy elements simulated realistic snow distributions.
- The proposed approach uses standard canopy parameters only and can thus be transferred to other model frameworks.

Abstract

Modelling spatiotemporal dynamics of snow in forests is challenging, as involved processes are strongly dependent on small-scale canopy properties. In this study, we explore how local canopy structure information can be integrated in a medium-complexity energy-balance snow model to replicate observed snow patterns at very high spatial resolutions. Snow depth distributions simulated with the Flexible Snow Model (FSM2) were tested against extensive experimental data acquired in discontinuous subalpine forest stands in Eastern Switzerland over three winters. While the default canopy implementation in FSM2 fails to capture the observed snow depth variability, performance is considerably improved when local canopy cover fraction and hemispherical sky view fraction are additionally accounted for (30% reduction in RMSE). However, realistic snow depth distribution patterns throughout the season are only achieved if effective temperatures of near and distant canopy elements are discerned, and if a mechanism to mimic preferential deposition of snow in canopy gaps is included. We demonstrate that by diversifying the canopy structure input in order to reflect respective portions of the canopy relevant to different processes, even a simple model based on widely used process parameterizations and canopy metrics can be applied for high-resolution simulations of the sub-canopy snow cover with just a few modifications. The presented approaches could be implemented in commonly used land surface models, allowing upscaling experiments and development of sub-grid parameterizations without necessitating complex high-resolution models.

1. Introduction

The large spatial overlap of forest and seasonal snow makes the sub-canopy snow cover a key control of eco-hydrological processes at high latitudes and in alpine regions (Lundquist et al. 2013; Trujillo et al. 2012). In these environments, accurate models are needed to predict potential effects of ongoing climate and vegetation changes in support of water resources management (Beniston 2003; Marty et al. 2017; Tape et al. 2006). However, forest snow dynamics are shaped by complex interacting processes that are controlled by the structure of the overhead canopy and thus display large spatial and temporal variation. Snow interception by the canopy (Hedstrom & Pomeroy 1998; Moeser et al. 2015b; Roth & Nolin 2019) and subsequent sublimation and unloading to the ground (MacKay & Bartlett 2006; Pomeroy et al. 1998), shading of shortwave radiation (Hardy et al. 2004; Malle et al. 2019; Musselman et al. 2012a) and emission of longwave radiation by the vegetation (Essery et al. 2008b; Pomeroy et al. 2009; Webster et al. 2016) all vary with canopy structure in specific ways and thus contribute to heterogeneous snow depth distribution patterns, which are difficult to replicate with models (Clark et al. 2011a).

The forest snow model inter-comparison project SNOWMIP2 (Essery et al. 2009; Rutter et al. 2009) evaluated 33 forest snow models differing in both process complexity and canopy implementation approaches. Major deficiencies of forest snow models were identified, and it was concluded that increased model complexity did not necessarily entail better performance (Rutter et al. 2009). Since then, the forest snow research community has come a long way: numerous measurement campaigns have generated a wealth of field data, comprising snow distribution observations (Dickerson-Lange et al. 2015; Harpold et al. 2014; Mazzotti et al. 2019a; Schneider et al. 2019), micrometeorological records (Mahat & Tarboton 2014; Roth & Nolin 2017) and distributed measurements at the level of individual processes (Lawler & Link 2011; Mazzotti et al. 2019b; Moeser et al. 2015b; Webster et al. 2016). Forest snow research has also substantially benefited from the increased availability of canopy structure information from a variety of remote sensing products (Ginzler & Hobi 2015; Harpold et al. 2014; Moeser et al. 2015a; Varhola & Coops 2013). As a consequence, many snow routines in hydrological and land surface models have been enhanced to incorporate more accurate representations of forest snow processes (Boone et al. 2017; Ellis et al. 2013; Gouttevin et al. 2015; Mahat & Tarboton 2014; Mahat et al. 2013; Sun et al. 2018). Yet in many cases, the canopy is represented as one layer whose energy balance is coupled to that of the snowpack (Broxton et al. 2015; Mahat & Tarboton 2012; Moeser et al. 2016; Musselman et al. 2012b).

Recent studies concerned with physically-based forest snow modelling have generally either focused on describing individual processes, or on implementing parameterizations of these processes into full snow cover models. In the former case, efforts to link process variability to canopy-structural variability at very small scales are common (Lawler & Link 2011; Musselman et al. 2012a; Webster et al. 2016). In contrast, studies evaluating the performance of full forest snow models have mostly been tested at the site scale only, using canopy parameters that represented effective spatial averages (Ellis et al. 2010; Gouttevin et al. 2015; Mahat et al. 2013). To date, few studies have incorporated local canopy structure into energy balance forest snow models to evaluate simulated variations across very small spatial scales: Musselman et al. (2012b) improved simulations of point-scale snowmelt dynamics by forcing the detailed snow-physics model SNOWPACK (Lehning et al. 2006) coupled to a 1-layer canopy with time series of direct-beam shortwave radiation transmissivity. Moeser et al. (2016) obtained realistic spatial snow-depth distributions (2m resolution) with the Factorial Snowpack Model (Essery 2015) by implementing a novel interception model that uses detailed canopy structure parameters (Moeser et al. 2015b). Broxton et al. (2015) introduced SnowPALM, a model specifically designed for distributed forest-stand simulations (1m resolution), which aims at capturing differences between under-canopy and near-canopy pixels. SnowPALM accounts for horizontal interactions between grid cells through explicit simulation of shading and wind-redistributed snowfall.

Broxton et al. (2015) further demonstrated the utility of meter-scale simulations for evaluating errors that arise when the non-linear forest snow processes are integrated over larger modelling units. With increasing availability of canopy structure information and computational resources, high-resolution modelling could enhance our understanding of inaccuracies inherent to common model applications (Essery et al. 2009; Sohrabi et al. 2019). Such model experiments should use process formulations that can be applied consistently throughout varying spatial scales. However, it is essentially unknown how well ‘standard’ medium-complexity models intended for and validated at the site scale are suited to replicate small-scale spatial snow variability that arises from complex processes.

In this study, we explore how a physically-based snow model with simple parametrizations of energy fluxes and a 1-layer canopy representation can be applied to yield meaningful high-resolution simulations (<10m). To this end we use a forest snow scheme that incorporates process parameterizations used in many land surface models. Specific objectives are:

1. To assess empirical relations between extensive snow depth and co-located canopy structure data, motivating the choice of local canopy parameters for modelling.
2. To evaluate how commonly used canopy structure representations can be adapted to allow realistic replication of observed snow depth distribution patterns.

3. To provide a framework for consistent and accurate model simulations of forest snow distributions from fine to coarser scales that will facilitate upscaling experiments.

This paper is structured as follows: Section 2 gives an overview of the available snow depth and canopy structure data and our modelling strategy. Experimental findings and modelling results are presented in section 3. As the design of each model version resulted from insights gained with the previous one, results are outlined and interpreted sequentially and unavoidably anticipate some discussion elements. Section 4 discusses the utility of our approach in a broader forest snow modelling context, while conclusions from this study are drawn in section 5.

2. Methods

2.1 Study sites and snow depth data

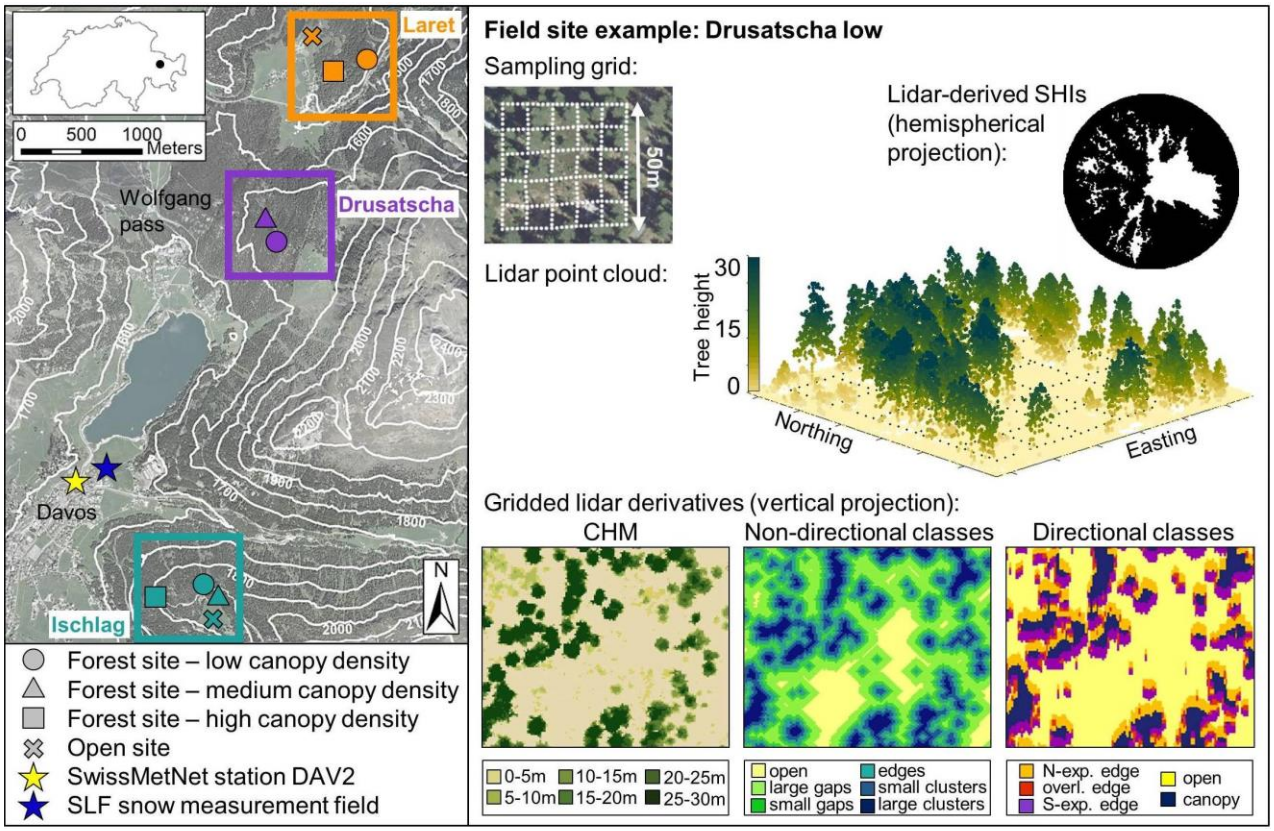

Figure 1: Left: Overview map of the field areas, locations of the automatic weather station and the SLF snow measuring field (left) in Switzerland. Right: Example of the Drusatscha low field site, including the sampling grid, a visualization of the lidar point cloud, and lidar-derived datasets (see section 2.2.): canopy height model (CHM), directional and non-directional pixel classification and synthetic hemispherical image (SHI).

Observational data come from discontinuous forest stands in the vicinity of Davos, Eastern Swiss Alps (Figure 1). The area is characterized by complex terrain and inner-alpine climate, with mean winter temperatures around -2 °C and an average precipitation of ~400mm during the winter half-year (October to March, MeteoSwiss, www.meteoswiss.admin.ch). Its subalpine forests are dominated by Norway spruce (*Picea abies*) ranging from new-growth to 45m in height. The seven study sites, grouped into three field areas Drusatscha, Ischlag and Laret

(Figure 1), were established for a long-term forest snow study and have been described in detail by Moeser et al. (2014). Canopy cover exhibited pronounced variability both between and within sites (hence the site tags ‘low, medium and high’), whereas terrain influences were minimal. Each site included six parallel 50m transects intersected orthogonally by six further transects to form a 50x50m grid. Metal poles at intersection points and nylon cord between these were installed to mark snow depth measurement locations every 2 m along the transects. Intersection points were georeferenced with a differential GPS (Trimble Geo XH 6000). Predetermining and marking measurement locations (276 points per site) was key to efficient data collection. Additionally, two reference open sites comprising a 100m transect each were established at the Laret and the Ischlag field areas.

Snow depth (HS) was surveyed bi-weekly during three winters (water year 2012-13 to 2014-15). Unfortunately, the sites Ischlag low and Laret high had to be abandoned in the last winter due to logging activities. Over the entire study period, 34 campaigns generated an unprecedented dataset of manual forest snow depth measurements including ca. 60,000 data points.

2.2 Canopy structure metrics

Canopy structure information was retrieved from a detailed lidar dataset (approx. 35 points per m^2) acquired in September 2010 with a helicopter-borne Riegl LMS Q560 sensor. Details on lidar survey parameters are outlined in Moeser et al. (2014) who used the dataset to develop their algorithm for the creation of synthetic hemispherical images by coordinate transformation (Figure 1). From their study, synthetic hemispherical images were available at all surveyed points of all our study sites. Point cloud data were also processed to obtain vertically projected gridded datasets (Figure 1). Canopy height models (CHMs) were computed for 200 x 200 m areas encompassing each site at a 0.5 m resolution following the approach proposed by Khosravipour et al. (2014). Based on LAStools software (https://rapidlasso.com/lastools/), their algorithm creates pit-free CHMs by merging partial CHMs corresponding to defined canopy height bands generated by triangulated irregular networks (TIN) interpolation. The canopy height models were further binarized based on a 2m threshold as in e.g. Harpold et al. (2014) and Currier et al. (2019). The resulting binary raster was input to the algorithm presented by Mazzotti et al. (2019a), which computes every pixel’s distance-to-canopy-edge (DCE) as well as distances to the north- and south-exposed canopy edges (NDCE, SDCE).

Based on these lidar derivatives, the four canopy structure parameters most commonly used in snow models (Varhola & Coops 2013) could be computed at each of the surveyed locations. They include:

- *Leaf area index (LAI):* the dimensionless ratio of one-sided needle leaf area per unit ground area (e.g. Chen et al. 1997). Note that in some literature vegetation area index (VAI) is used instead, which may also include other vegetation elements such as stems and branches.
- *Sky-view fraction (V_F):* the visible portion of sky in the hemispherical field of view seen from a specific point, weighted by the sine of elevation angle (e.g. Essery et al. 2008b).
- *Canopy cover fraction (CC):* the ratio of area covered by the vertical projection of the canopy relative to ground area in a two-dimensional bounding box (e.g. Mazzotti et al. 2019b).

- *Mean canopy height (mCH):* the average height of the canopy elements in a two-dimensional bounding box (e.g. Varhola & Coops 2013).

LAI and V_F were derived from the synthetic hemispherical images. We use LAI values computed by Moeser et al. (2014) who applied standard approaches for calculation of LAI from real hemispherical images (Miller 1967) implemented in the free software Hemisfer (Schleppi et al. 2007). Sky-view fraction was calculated according to Essery et al. (2008b). CC and mCH metrics were derived from the canopy height model over circular domains of varying radii (1-20m) around the point of interest (i.e. CC_5 for a radius of 5m, mCH_X with a radius of x m). Additionally, the DCE, NDCE, and SDCE grids served to characterize each point's position relative to its surrounding canopy structure. For this purpose, we applied the two classifications which group pixels that are located within similar canopy structure by defining categories based on DCE thresholds (Mazzotti et al. 2019a), or alternatively on NDCE and SDCE thresholds (Figure 1). Pixels were categorized into large and small canopy gaps, canopy edges, and small and dense clusters of canopy elements according to their DCE value ('non-directional classification'). Additionally, they were classified as open or canopy pixels, north- and south-facing edge or overlapping edge pixels based on their NDCE and SDCE values ('directional classification').

2.3 The Flexible Snow Model (FSM2)

The Flexible Snow Model (FSM2) used in this study is a recent upgrade of the Factorial Snow Model (FSM; Essery 2015). FSM is an open-source energy balance snow model of medium complexity, i.e. a 'Type 2' model in the classification proposed by Vionnet et al. (2012), and was originally developed for point simulations at open sites. Implemented as a multi-model framework (e.g. Clark et al. 2015; Essery et al. 2013), FSM includes two alternative parameterizations for five snow properties and processes, denoted as options 0 ('simple') and 1 ('more complex'). For the purpose of this study, we considered only one model configuration, with option 1 chosen for all snow properties and processes (snow albedo, snow density, snow compaction, and snow hydrology) except for turbulent exchange, as the assumptions underlying the stability correction implemented in FSM are likely to be violated in discontinuous forests (Conway et al. 2018).

FSM2 offers the addition of a one-layer canopy implementation, which is common in land-surface models and makes it applicable to forested areas. Standard parameterizations of canopy processes applied in established models such as CLASS (Bartlett et al. 2006), ISBA (Boone et al. 2017) and CLM (Oleson et al. 2013) are included; see the Appendix for a description. At every modelled forest location, FSM2 requires information on site characteristics in terms of canopy parameters. By default, only vegetation area index (VAI, c.f. Section 2.2) and canopy height (h_c) are needed, while transmissivity τ and vegetation fraction f_v are computed internally as functions of VAI. However, f_v and τ can also be specified as optional user inputs if specific values are available. In the context of local-scale modelling, this versatility permits integration of canopy structure metrics that incorporate different viewing perspectives and / or portions of the canopy, depending on what is relevant for the process in question.

The model used by Moeser et al. (2016) constituted an unpublished precursor of FSM2. Since then, the model code has undergone substantial re-structuring and replacement of some process parameterizations. Recently, FSM2 was applied in a study by Magnusson et al. (2019) on scale errors for simulations ranging between 1 and 50 km. This paper uses FSM2 version 2.0.1 (doi: 10.5281/zenodo.2593345).

2.4 Meteorological driving data

FSM2 is driven by meteorological input data including incoming short- and longwave radiation, rain- and snowfall rates, air temperature, relative humidity, wind speed and surface air pressure. All required meteorological data were obtained at hourly resolution from the automatic weather station in Davos (DAV2), operated by MeteoSwiss (www.meteoswiss.admin.ch, Figure 1) and located within 4 km of all sites.

Total precipitation, measured by a heated gauge, was partitioned into solid and liquid components (P_S and P_L) applying the same partitioning function as in Magnusson et al. (2014) and Moeser et al. (2016):

$$P_S = P_{tot} \frac{P_{corr}}{1 + e^{\frac{T_a - T_P}{m_P}}}$$

P_{corr} denotes an undercatch correction factor for solid precipitation, which was calibrated on a seasonal basis by comparing measured precipitation to bi-weekly surveys of snow water equivalent (SWE) at the nearby SLF measurement field (Figure 1) during cold periods (T_a < 0°C). Values ranging from 1.3 (2013/14) to 1.4 (2014/15) are in good agreement with those reported in other studies in the same region (e.g. Egli et al. 2009; Wever et al. 2014). The parameters T_P = 1.04 °C (threshold temperature where P_S = P_L = 0.5) and m_P = 0.15 °C (temperature range corresponding to mixed precipitation) were calibrated on FSM2 results at the open sites and are consistent with Magnusson et al. (2014) and Moeser et al. (2016).

Secondary precipitation correction factors specific to each field area were applied to account for the strong horizontal precipitation gradient arising from topographic conditions, which generally yield more snow at the field areas Laret and Drusatscha north of Wolfgang pass (Figure 1). These factors were computed for each season and field area individually as the ratio of peak SWE at the respective open field area to peak SWE measured at the SLF snow field, similar to Vögeli et al. (2016). Furthermore, the standard atmospheric lapse rate of -0.65°C/100m of elevation gain was applied to the air temperature time series to account for elevation differences between the sites. All other data (incoming radiation, relative humidity, wind speed and air pressure) were unchanged for all sites. Simulations at the open areas Laret, Ischlag and Davos were performed to ensure satisfactory input data quality and model performance independent of canopy-induced processes.

2.5 Model application and evaluation strategy

FSM2 was chosen for this study because it uses standard process parameterization approaches (c.f. Section 2.3). Moreover, its flexible structure and canopy parameters input offer a convenient testbed for alternative canopy structure representations. We explored different ways to leverage the experimentally available canopy structure data (LAI, V_F, CC_X, mCH_X) as canopy input to FSM2 (VAI, h_c, f, τ) without fundamental changes to the process parameterizations used in the model. The four alternative model versions are briefly introduced in the following:

- *FSM2-A:* This constitutes the default version of FSM2. Leaf area index LAI and mean canopy height mCH_5 were used as the only canopy input parameters for VAI and h_c, while f_v and τ were estimated by the parameterizations implemented in FSM2. As LAI from synthetic hemispherical images is always non-zero, mCH_5 values were set to a minimum of 2m (i.e. the threshold used to binarize the CHM) to ensure parameter compatibility.

- *FSM2-B:* Here, we attempted a more accurate representation of local canopy conditions relevant to each process by providing additional user inputs for f_v and τ in terms of local canopy closure CC_5 and sky view fraction V_F. This allowed us to give more weight to local canopy information for processes such as interception, while maintaining the overall canopy layout for processes such as shortwave transmission. As in FSM2-A, h_c was given by mCH_5. However, as LAI values obtained from hemispherical imagery integrate canopy information over a large fetch, VAI was instead determined with a linear function scaling with CC_5 and mCH_5 to achieve a more local approximation:

$$VAI = max(LAI) \cdot CC_5 \cdot \frac{mCH_5}{max(mCH_5)}$$

- *FSM2-C:* This version introduced separate treatment of near and distant canopy elements in the energy balance. VAI, f_v and h_c were determined as in FSM2-B, but transmissivity was split into non-local and local components *fsky* and τ. The parameter *fsky* was originally implemented in FSM2 to optionally account for terrain shading at non-forested sites. In our application to forest simulations, we leveraged the same approach to discern near and distant canopy elements, with (1-*fsky*) representing distant canopy and terrain and (1- τ) denoting near canopy. It follows that τ and *fsky* are constrained by total hemispherical sky view, i.e. $\tau \cdot fsky = V_F$. We combined V_F and CC_5 data to estimate *fsky* and τ as follows:

$$\tau = 1 - CC_5$$

$$f_{sky} = \frac{V_F}{\tau}$$

By using CC_5 to define local canopy components, we could avoid introducing an additional canopy parameter. In those few cases where this led to *fsky* > 1, all canopy was treated as local, i.e. *fsky* = 1 and $\tau = V_F$. The temperature of distant canopy and terrain was assumed to equal air temperature, while only near canopy elements were involved in the coupled snow and canopy energy balances, with implications for radiative transfer. Moreover, f_v was replaced by (1 - V_F) for weighing the turbulent transfer coefficient between the canopy air space and the ground.

- *FSM2-D:* In this version, all canopy parameters were computed as in FSM2-C. In addition, a simple local precipitation scaling was introduced to mimic preferential deposition of precipitation (Lehning et al. 2008) and redistribution of snow intercepted by the canopy (Mahat & Tarboton 2014):

$$S_{f,corr} = S_{f,raw}\,(1.1 - 0.2 \cdot CC_5),$$

where the limits of this rescaling (+/- 10%) were motivated by Mahat and Tarboton (2014).

The approaches included in each model version were motivated by results from the previous one, which is why further details on the above model choices will be discussed alongside results in section 3.2. The four versions were run at all seven sites for the three winters

(October 1st to May 31st; 2012/13-2014/15), yielding a daily time series of snow depth (HS) for 276 points per site, i.e. 1932 points in total.

Model performance was evaluated by comparing simulations at the grid intersection points of each field site to observed values aggregated over a 5m radius (i.e. 9 measurements per validation point, 16 validation points per site). This choice is discussed in section 3.1, but it matches the canopy structure evaluation fetch of the parameters CC_5 and mCH_5 used in the model. We assessed the root mean square error (RMSE) and the mean absolute error (MAE) of snow depth, the mean absolute error of the standard deviation of snow depth within each field area (STDerr), Pearson's correlation coefficient (R) between observed and simulated HS, and the Kling-Gupta efficiency (KGE; Gupta et al. 2009). The KGE statistic combines a correlation, a bias and a variability component, and has been applied to snow model performance assessment by Magnusson et al. (2015). These goodness-of-fit metrics were computed separately for each field area and survey date.

3. Results

3.1 Empirical relationships between snow distribution and canopy structure

Correlations between snow depth and local canopy structure metrics

Analyzing correlations between snow depth and canopy structure metrics served to identify canopy parameters to potentially include in FSM2. We computed correlation coefficients (Pearson's R) between point snow depth measurements and all canopy parameters, including CC and mCH evaluated with varying radii, for all sites and survey dates. The temporal evolution of these correlations is shown in Figure 2 (left panel) based on data from Laret low as an example. A summary of correlation statistics at each site is provided in the right panel, where canopy metrics were ranked by their R values for each individual campaign and the average rank over the entire study period is reported for each canopy metric and site. Two general trends emerge: First, the stronger correlations between snow depth and metrics that are based on a small evaluation fetch (up to 5m) highlight the control of small-scale canopy structure on snow distribution. Second, CC-based parameters exhibit the strongest correlations with snow depth, while correlations to V_F and LAI are remarkably weaker, suggesting that high-resolution modelling may benefit from incorporating a local CC metric. Correlation patterns further show strong temporal consistency, with generally higher R values during the accumulation period than during the ablation period. This may suggest that a single canopy parameter alone cannot accurately describe snow distribution once ablations processes have started to superimpose accumulation patterns.

Our choice to implement CC and mCH based on a 5m evaluation fetch (i.e. CC_5, mCH_5) into FSM2 is also motivated by the data shown in Table 1, reporting correlation coefficients between CC based on different radii and HS aggregated over the same spatial unit. Contrary to results in Figure 2, correlations here improve for larger evaluation fetches; this is due to averaging snow depth data, which smooths out the scatter intrinsic to the observational data generating from random effects such as local ground roughness. Such random variability cannot be captured by the model. We therefore assessed the 5m spatial scale to be the best tradeoff between correlation strength, sample size and aggregation of observational data. At the same time, this scale is compatible with the experimental design of our sites, as aggregated points could be centered around transect intersections.

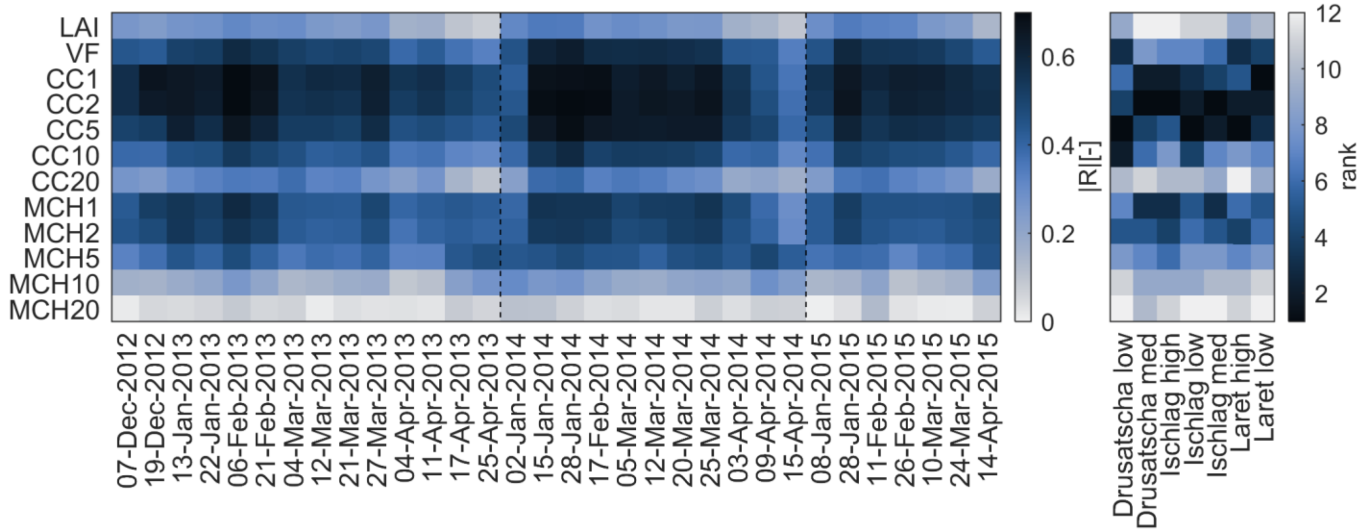

Figure 2: Correlations between local snow depth and different canopy structure variables. Left: At the Laret low site, for all individual campaigns throughout three seasons (dashed lines mark the separation between seasons). Right: At all sites, average rank of R over the entire study period. Note that correlation coefficients are reported as absolute values.

Table 1: Maximum and average correlation coefficients between canopy closure (CC) computed over varying evaluation fetches and snow depth (HS) aggregated over the same spatial scale. R max is the maximum correlation found for any site or survey date and R mean is the average over all sites and campaigns. The sample size on which these statistics are based is also included.

CC and HS evaluation fetch	**1m**	**2m**	**5m**	**10m**	**20m**
R max	-0.79	-0.85	-0.95	-0.99	-0.97
R mean	-0.58	-0.65	-0.82	-0.89	-0.76
Sample size	1932	672	112	28	3

Linking snow depth patterns and spatial canopy arrangement

To derive expected model behavior, we further investigated how the spatial organization of the canopy, described in terms of DCE-based directional and non-directional classifications, affects snow depth patterns. Median snow depths within each pixel class were compared for both the non-directional (Figure 3, left) and the directional (Figure 3, right) classifications. Differences in snow depth between non-directional DCE classes are pronounced over the entire course of the season(s) and are much more distinct than differences between snow depths at canopy edges facing opposite aspects (red and purple lines on the right panel of Figure 3). Data from the Ischlag high site are shown as an example, but these patterns are generally consistent for all sites and seasons. This finding conforms with Mazzotti et al. (2019a), who came to the same conclusion based on forest snow distribution data derived from airborne lidar; however, data presented here offer a much larger temporal range. While several studies have highlighted the impacts of directional effects such as aspect-dependent irradiance and wind-driven preferential deposition on snow distribution (Broxton et al. 2015; Currier & Lundquist 2018; Hiemstra et al. 2006), these effects are mainly observed along the edges of forest stands and of large forest gaps. In contrast, our sites reside within discontinuous forest stands characterized by relatively small gaps (<2H, c.f. Lawler & Link, 2011). Our data attest to the prevalence of non-directional effects over directional ones at such within-stand locations. This suggests that within discontinuous forest, even a model with a simple canopy implementation may be sufficient to capture the principal links between snow depth and canopy structure pattern.

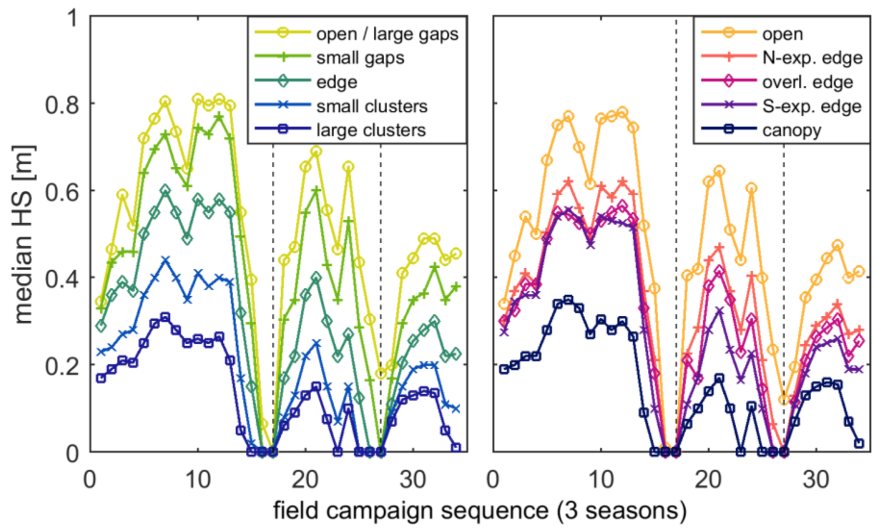

Figure 3: Temporal evolution of observed average snow depth (HS) for different pixel classifications (dashed lines mark the separation between seasons, 2012/13 to 2014/15). Left: Non-directional classification based on distance-to-canopy-edge (DCE) threshold; Right: Directional classification aiming at delineating edges of opposite aspect based on NDCE and SDCE thresholds.

3.2 Simulations of spatiotemporal snow depth distribution dynamics with alternative canopy representations

The following sections outline and discuss results obtained with the four model versions individually, where the sequential order reflects the learning process that drove our model development. Different aspects of our results are presented in four separate figures, which are repeatedly referred to as we interpret and discuss the results of every model version separately. We briefly introduce these figures here for context: Figure 4 presents the temporal evolution of snow depths simulated by the four FSM2 versions at the 16 intersection points of the Drusatscha low site alongside corresponding observations. CC_5 is used as a color scale, where each line represents one of the 16 intersection points with its unique CC_5 value and serves to illustrate the variation of snow depth with local canopy structure. In contrast, Figure 5 and Figure 6 show temporal snapshots of observed and modelled snow depth distributions around peak of winter for two different sites and seasons, helping to visualize spatial snow depth patterns and their position relative to the canopy. The corresponding canopy height models reveal strong differences in canopy structure between these two examples. Lastly, observed and simulated snow depths at all field sites are directly compared at individual locations in Figure 7, from a survey in the accumulation period (left panels) and one in the ablation period (right panel).

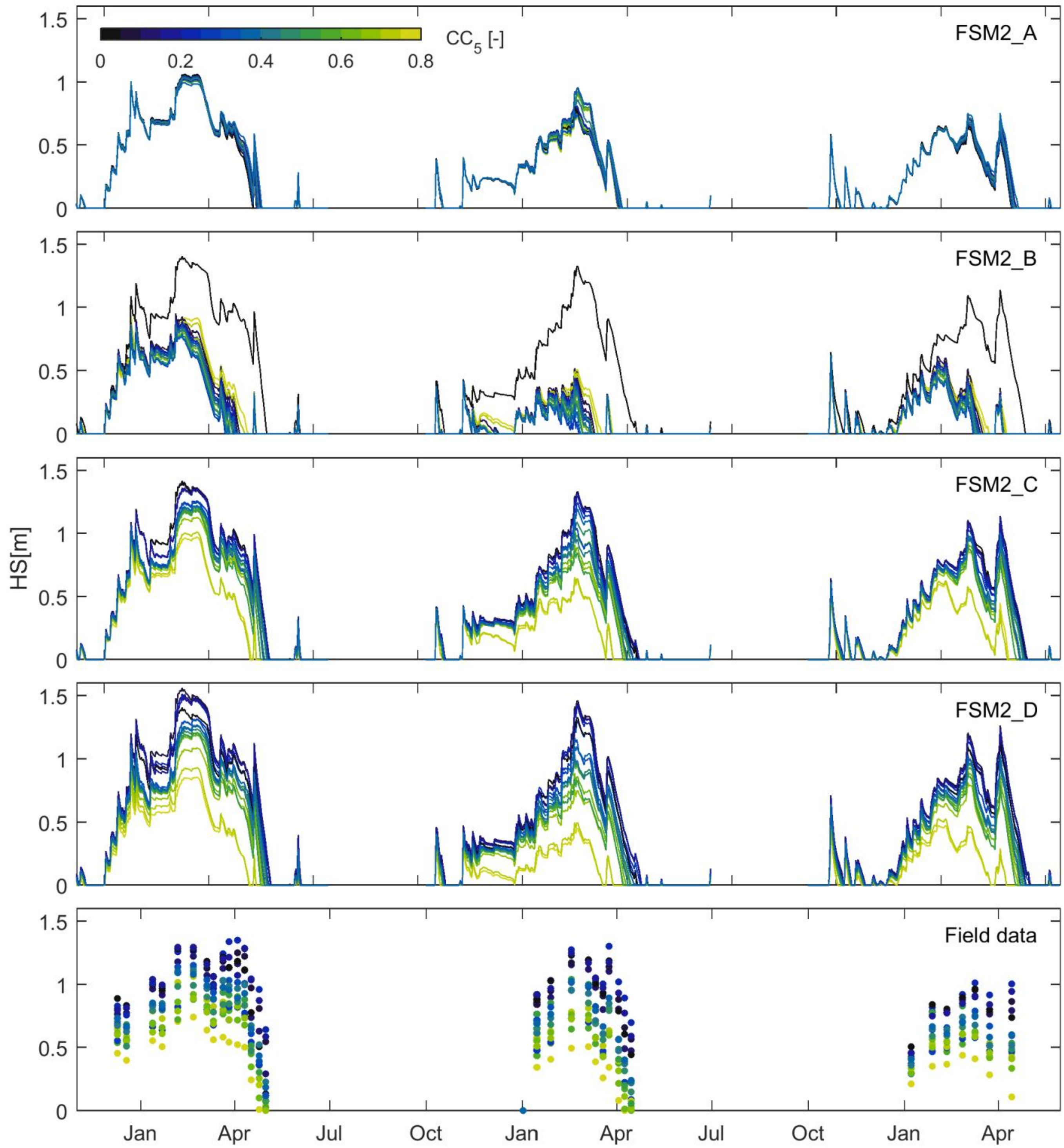

Figure 4: Temporal evolution of simulated (FSM2-A to D) and observed (field data) snow depth (HS) at the 16 intersection points of the Drusatscha low site. The color scale visualizes CC_5 at the points.

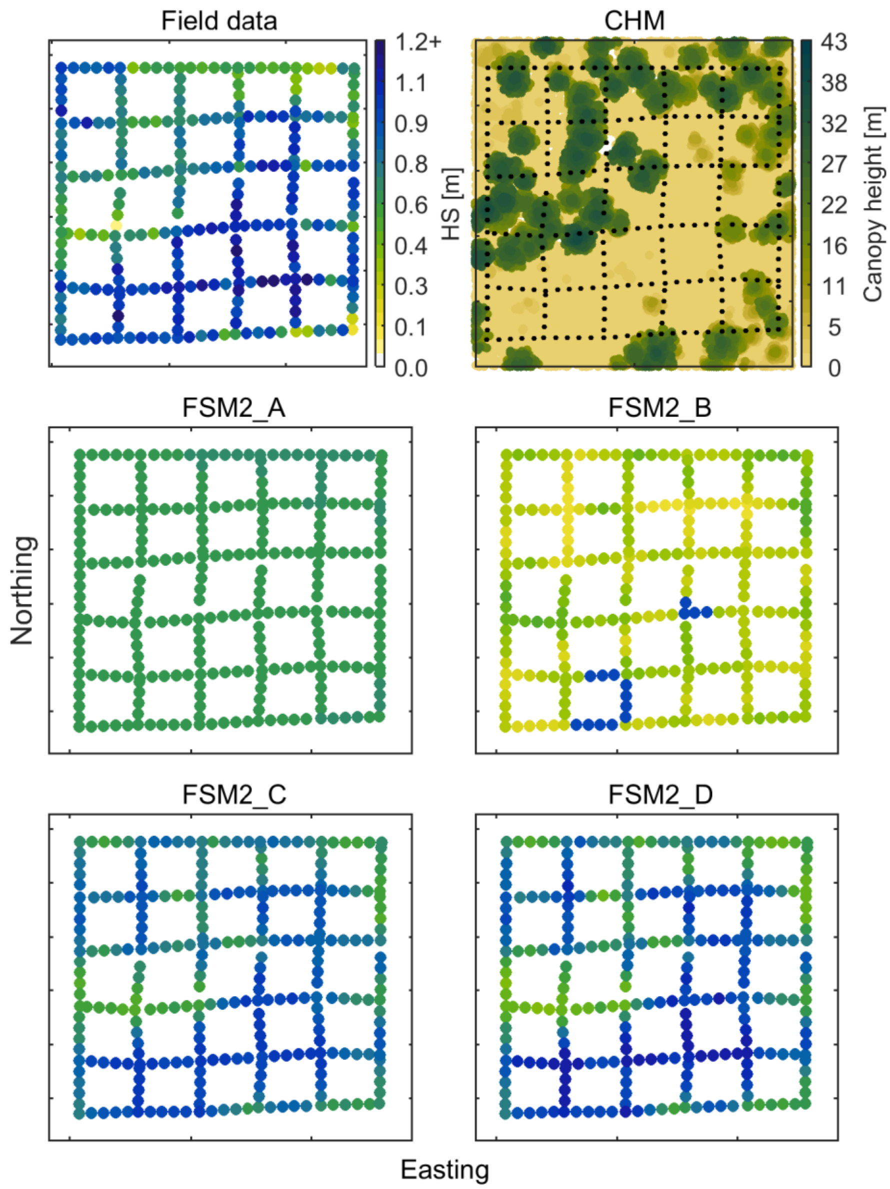

Figure 5: Spatial snow depth (HS) distribution observed at the Drusatscha low site on 12 March 2013 (upper left), co-located canopy height model (CHM), and model results for the same date obtained with the four FSM2 versions (lower 4 panels).

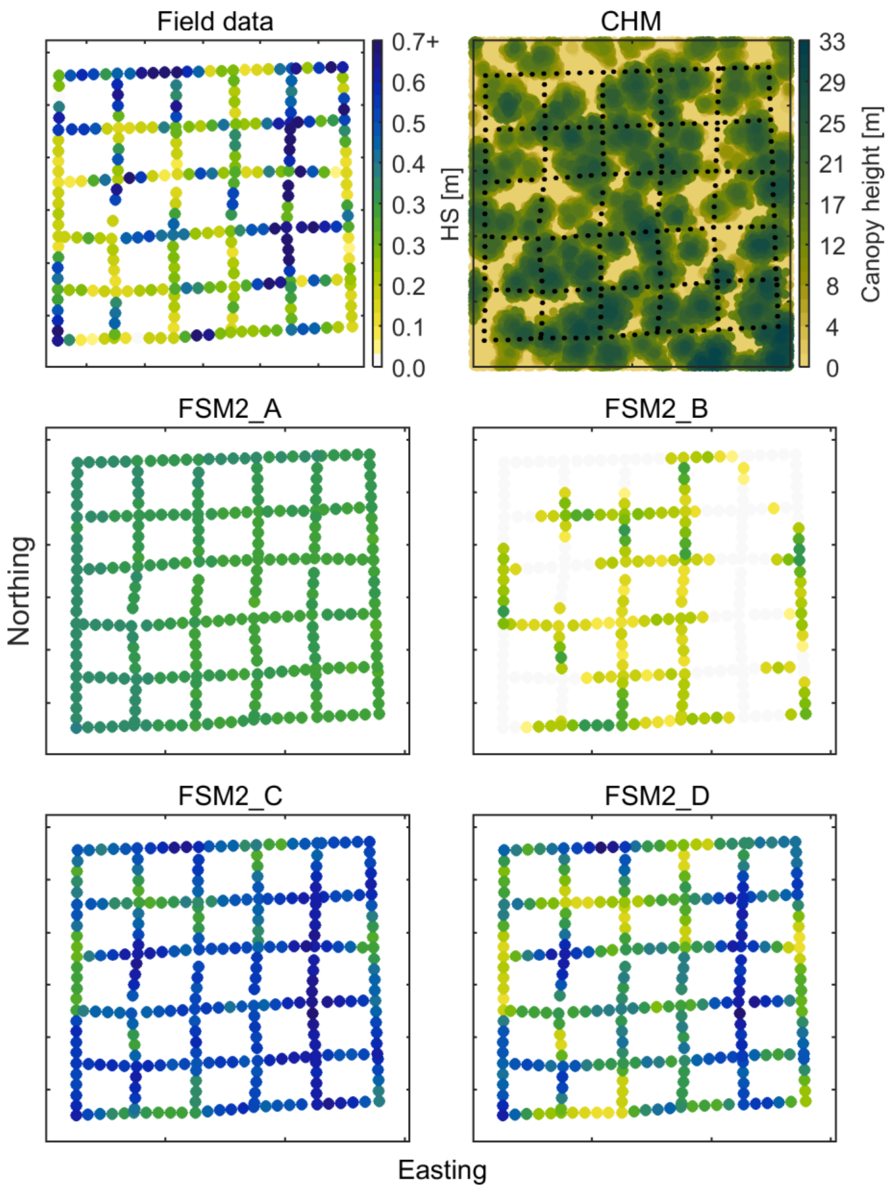

379

380 **Figure 6:** Same panels as in Figure 5 but showing data from Ischlag high on 5 March 2014.

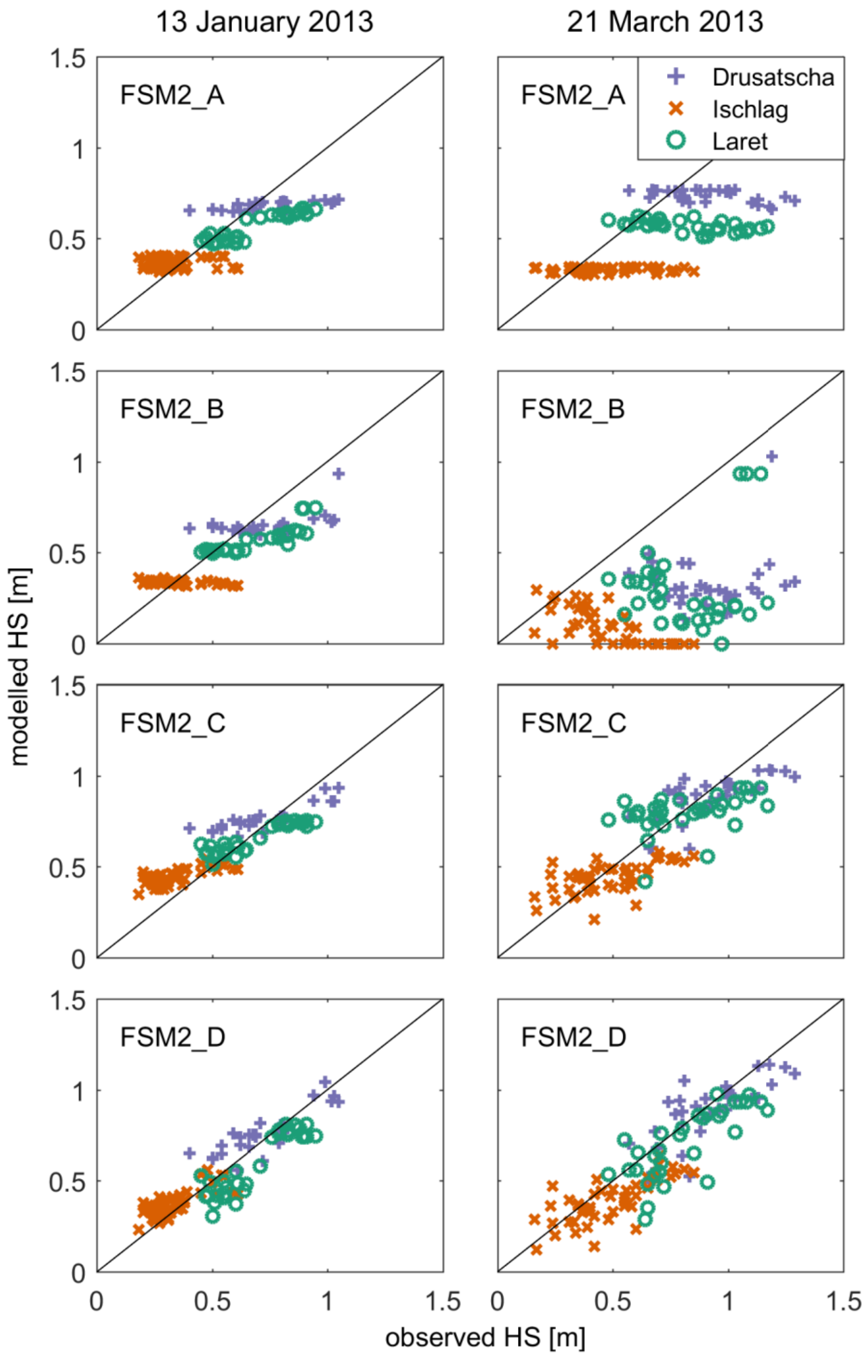

Figure 7: Comparison of observed snow depths (HS) at the 16 intersection points of all sites and model results obtained by the four FSM2 versions, for a campaign in the accumulation season (left) and one during the ablation season (right).

FSM2-A: Default canopy implementation underestimates spatial variability

The default FSM2 version, FSM2-A, strongly underestimates the spread in snow depth at points characterized by varying canopy cover fraction throughout the whole simulation period (Figure 4, first panel). As a consequence, simulated snow depth distributions at peak of winter are homogeneous, regardless of whether strong local differences in canopy density exist within the site or whether the site features low canopy-structural variability (Figure 5 vs. Figure 6, center left panels). Simulated HS values therefore poorly match individual observations during both the accumulation and the ablation period (Figure 7, first row).

These results suggest that canopy structure variability is not adequately captured by standard LAI estimates and canopy height alone. At the local scale, different processes involved in the snow mass and energy balances are affected by different portions of the canopy (Moeser et al. 2015a), but the limited canopy structure input in FSM2-A does not account for these differences. In particular, LAI estimates based on hemispherical photography are inappropriate for characterizing local canopy in gaps: LAI is always non-zero even when no canopy is present directly overhead. Unavoidably, this leads to overestimations of interception in gaps, creating comparably homogeneous snow depth distribution as a consequence (Moeser et al. 2016). This example illustrates issues arising from the application of parameterizations developed at the stand scale (such as the Hedstrom & Pomeroy (1998) interception model) to simulations at the point (or meter) scale. Achieving successful process representation at very small scales may require diverse canopy structure input to allow distinction between overhead and surrounding canopy. Respective approaches have been implemented by Ellis et al. (2013) and Broxton et al. (2015) to enable simulations at gap locations that are sheltered and shaded by the canopy but have no interception.

FSM2-B: Default inclusion of local parameters entails shortcomings in both accumulation and ablation processes

To address issues identified with FSM2-A, the canopy parameterization strategy applied in FSM2-B attempted to diversify the canopy structure input, with the aim of representing the different processes by using canopy parameters that incorporate a spatial scale relevant to those processes. By providing FSM2 with locally measured inputs of CC_5, V_F and mCH_5, simulated interception could be controlled by the overhead canopy (CC_5, vertical perspective). At the same time, radiation transfer remained affected by surrounding canopy elements (V_F, hemispherical perspective).

Including additional forest structure information changed simulation results dramatically, but not generally for the better (Figure 4, second panel). Despite improved representation of local interception, the spread in HS is still underestimated during the accumulation period (Figure 7, second row left). The resulting snow depth patterns at peak of winter are still hardly visible (Figure 5, center right panel) or even reversed compared to observations (Figure 6, center right panel). The model melts snow too early in general and in gaps in particular. This resulted in consistent underestimations of snow depths during ablation (Figure 7, second row right).

Combining canopy parameters that integrate different perspectives entails potential problems that are best illustrated by considering the single point with consistently the highest accumulation and latest melt (dark blue line in Figure 4, second panel), the only intersection point with CC_5 = 0 (i.e. within a large gap) at the Drusatscha low site. The much faster melt of points characterized by a small CC_5 (other blue lines in Figure 4) reveals a discontinuity in the model at the transition from zero to non-zero CC_5 values (for equal V_F), which is a consequence of model structure: while shortwave radiation is attenuated by the same transmissivity $\tau = V_F$ in both cases, coupled energy balances of canopy and sub-snow require a canopy cover fraction (i.e. a non-zero f_v). Where this is not fulfilled, i.e. for $CC_5 = 0$, fluxes resulting from the energy balance equations, for instance longwave radiation enhancement, are completely eliminated. In contrast, longwave radiation is dictated by V_F at locations with $CC_5 > 0$, where rapid snowmelt indicates too high sub-canopy energy input. As shown by Gouttevin et al. (2015), this known shortcoming of 1-layer canopy models is likely due to an overestimation of effective canopy temperatures.

These results highlight that given the interplay between energy balance components, it is important that parametrizations of individual processes be evaluated within the full context of an energy balance model. Canopy gaps characterized by $CC_5 = 0$ and $V_F < 1$ are frequent in forest stands, contributing substantially to forest snow spatial variability (Dickerson-Lange et al. 2015; Mazzotti et al. 2019a; Murray & Buttle 2003; Sun et al. 2018), but FSM2-B fails to correctly capture snow cover dynamics at these locations, with shortcomings both in the accumulation and the ablation periods (Figure 7, second row). These were sequentially addressed in the two following model versions.

FSM2-C: Distinction between near and distant canopy elements improves simulated energy exchange

The distinction between local and non-local canopy elements implemented in FSM2-C specifically tackled the discontinuity in canopy gaps identified in FSM2-B. By accounting for distant canopy elements with vegetation temperature given by air temperature and independent of the canopy energy balance, longwave radiation enhancement can take effect even at locations with $CC_5 = 0$. At the same time, the dissimilar canopy temperatures of near and distant elements dampen the impact of too high vegetation temperatures for locations with $CC_5 > 0$. Indeed, this approach eliminated the discontinuity effectively, delayed snowmelt in canopy gaps relative to dense canopy (Figure 4, third panel), and improved the match between simulations and observations, both at the level of snow distribution patterns (Figure 5 and Figure 6, lower left panels) and individual values, especially later in the season (Figure 7, third row).

The 1-layer canopy models fail to represent shading of the lower canopy by the upper canopy, which is why multi-layer canopies have been proposed to arrive at more realistic estimates of effective canopy temperatures (Gouttevin et al. 2015). With the presented approach, the limitations associated with a 1-layer canopy could be circumvented without a considerable increase in model complexity. Although the proposed weighting based on CC_5 is certainly simplistic, it is justified from a process perspective: based on measurements of incoming sub-canopy longwave radiation, Webster et al. (2016) showed that the approximation of effective vegetation temperature by air temperature gained accuracy with increasing distance from the canopy. Distance based weighting of longwave radiation emissions from trees is also implemented in SnowPALM (Broxton et al. 2015). The relative contributions of sky and canopy to incoming longwave radiation are dictated by sky-view fraction, but canopy skin temperature is weighted by a function with length scale parameters calibrated on snow distribution. Their longwave radiation parametrization is briefly mentioned in the appendix but not discussed in their study, yet its conceptual similarity to our approach is noteworthy, and it is conceivable that this parameterization also contributed to the successful representation of spatial snow cover variability achieved with SnowPALM.

FSM2-D: Redistribution of canopy snow enhances variability during accumulation

Local variations in canopy snow interception generate spatial variability of snow on the ground during accumulation, but it is the fate of the intercepted snow that ultimately determines whether this variability persists over time. Unloading snow from the canopy generally involves some degree of horizontal redistribution and may even exacerbate spatial variability (Mahat and Tarboton 2014). Within a 1-D model, however, snow is typically unloaded at the location where it is intercepted, diminishing variability created by interception (e.g. Moeser et al. 2016). Disparities between snow depth in canopy gaps and under-canopy locations can be further enhanced by preferential deposition (Lehning et al. 2008), which likely occurs as a result of modified near-surface flow fields by the canopy and reduced wind speeds as a consequence (Roth & Nolin 2017). Both redistribution of intercepted snow and preferential deposition are difficult to observe, have not been quantified to date and are not usually included in forest snow models.

The precipitation scaling implemented in FSM2-D, suggested to mimic preferential deposition and redistribution processes, effectively increases snow depth spread during accumulation without requiring horizontal coupling (Figure 4, fourth panel; Figure 7, fourth row left). Spatial differences were further facilitated by slightly increasing the canopy snow holding capacity (motivated by the fact that the default value taken from literature has been suggested based on stand-scale studies) as well as the residence time of snow in the canopy (allowing sublimation to be active for longer). The resulting snow depth patterns match observations very well even at a site with little variability in canopy structure (Figure 5 and Figure 6, lower right panel), while the good results achieved with FSM2-C in the ablation period remain unaffected (Figure 7, lower right panel). For better visualization of resulting forest snow patterns, two animations showing a distributed simulation at the sites Drusatscha low and Ischlag low over the entire study period are included as supplementary material (Text S1, Movies S1 and S2).

Underestimation of spatial variability during accumulation has been identified in prior studies and tackled in different ways. Moeser et al. (2016) successfully simulated spatial patterns of canopy interception, but additionally modified the parameterization of canopy snow sublimation implemented in FSM2 to arrive at equally distinct below-canopy snow depth patterns. While the resulting sublimation rates were sufficiently high to preserve these patterns, potential impacts on other energy fluxes were not addressed in their study. Broxton et al. (2015) implemented wind-redistributed snow according to Winstral et al. (2002), introducing additional model parameters calibrated on distributed snow depth data. In contrast, constant precipitation correction factors were applied to under-canopy areas by Mahat and Tarboton (2014). Our precipitation scaling function attempts to reconcile these approaches by including a dependency on small scale canopy structure without increasing the number of canopy structure parameters involved.

3.3 Model performance metrics

Qualitative results presented in the previous section translate into goodness-of-fit metrics (Figure 8) that quantify the strong differences in model performance of the four FSM2 versions. The values shown in Figure 8 represent averages of the respective metrics over the three field areas for each individual survey date. Relative to the default version FSM2-A, deteriorated performance metrics are found for FSM2-B, with RMSE increasing by 52% (from 0.21m to 0.32m) and MAE by 71% (0.17m to 0.29m) on average. In contrast, model performance is improved considerably by the modifications introduced in version FSM2-C. RMSE and MAE are reduced considerably for both FSM2-C and FSM2-D, by 25% (0.16m, 0.13m) and 30% (0.14m, 0.11m), respectively. The improvements in model spread achieved with FSM2-D are reflected in a very small error in standard deviation (0.035m averaged over all campaigns), which is only 32% of the error found for FSM2-A (0.108m). Similarly, the slightly negative Pearson's R resulting for FSM2-A (-0.15) transforms into a strong positive correlation (0.73) for FSM2-D. These performance metrics are slightly better than for FSM2-C (STDerr = 0.052m; R = 0.69) due to the skill of FSM2-D to capture HS variability during the accumulation season. However, temporal differences are evident even in the case of FSM2-D. The best model performance is achieved around peak winter (up to R max = 0.86), while model deficiencies are larger early in the season and towards the end of the accumulation period (R min = 0.3). This could partly be due to inaccuracies in the model driving data and the function used to partition precipitation components. The smaller signal-to-noise ratio of the validation data in these periods further favors lower (apparent) model performance.

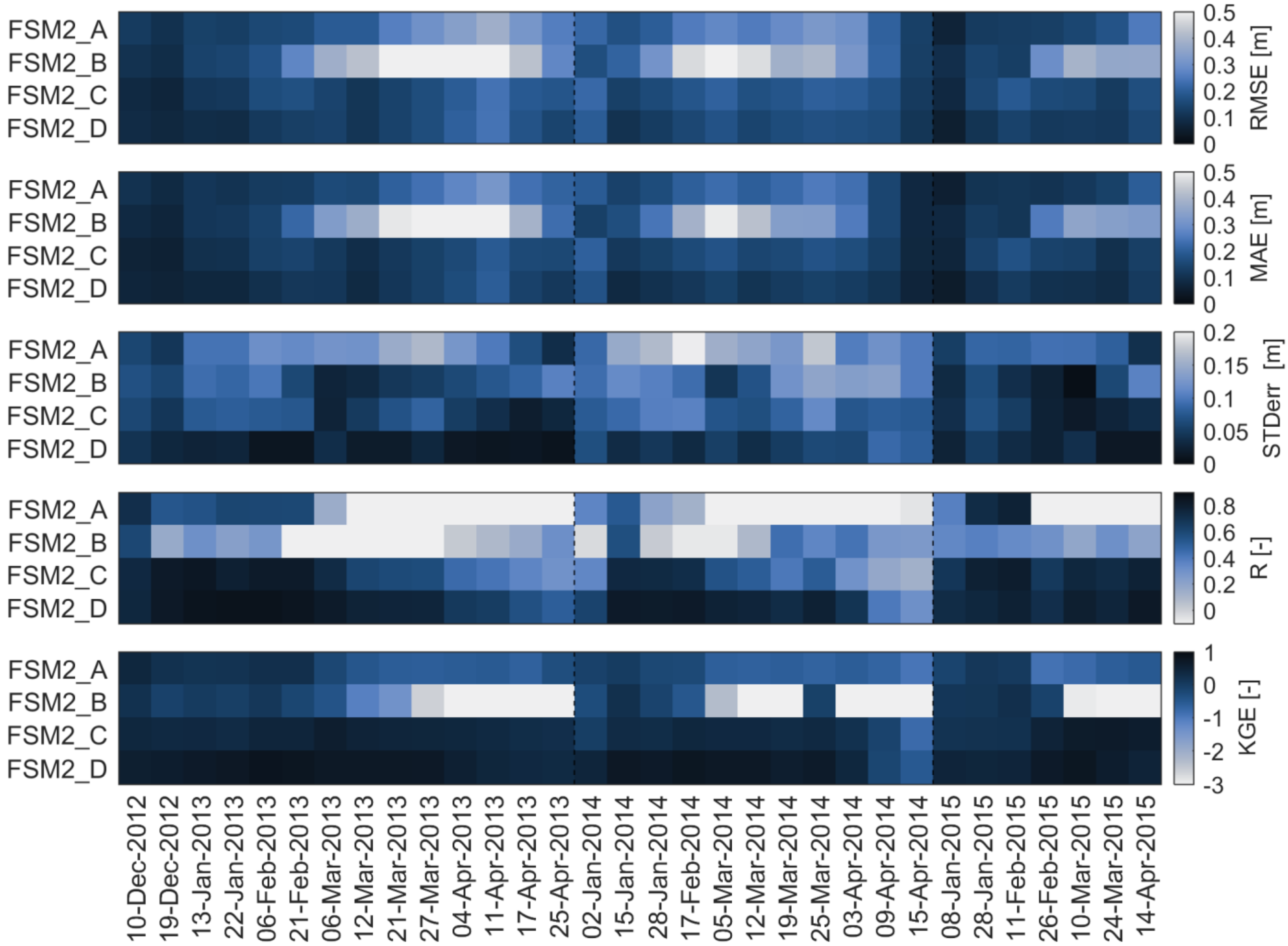

Figure 8: Temporal evolution of the five goodness of fit measures (one panel each) computed over all field areas for the four FSM2 versions.

The Kling-Gupta efficiency combines the aspects quantified by all other goodness-of-fit metrics. As expected, FSM2-C and FSM2-D clearly outperform FSM2-A and FSM2-B, and FSM2-D exhibits slightly improved performance relative to FSM2-C. For FSM2-D, KGE averaged over all campaigns amounts to 0.54 and maximum KGE to 0.80, while FSM2-A features a negative average KGE of -0.34. Lastly, the benefits of model performance improvements obtained with FSM2-D can be seen from the temporal evolution of the coefficient of variation of snow depth (CV; Figure 9). The CV is an important variability descriptor, applied e.g. in the parametrization of snow cover depletion curves (Liston 2004; Luce & Tarboton 2004) and FSM2-D arrives at the most accurate estimates of the CV metric throughout the season.

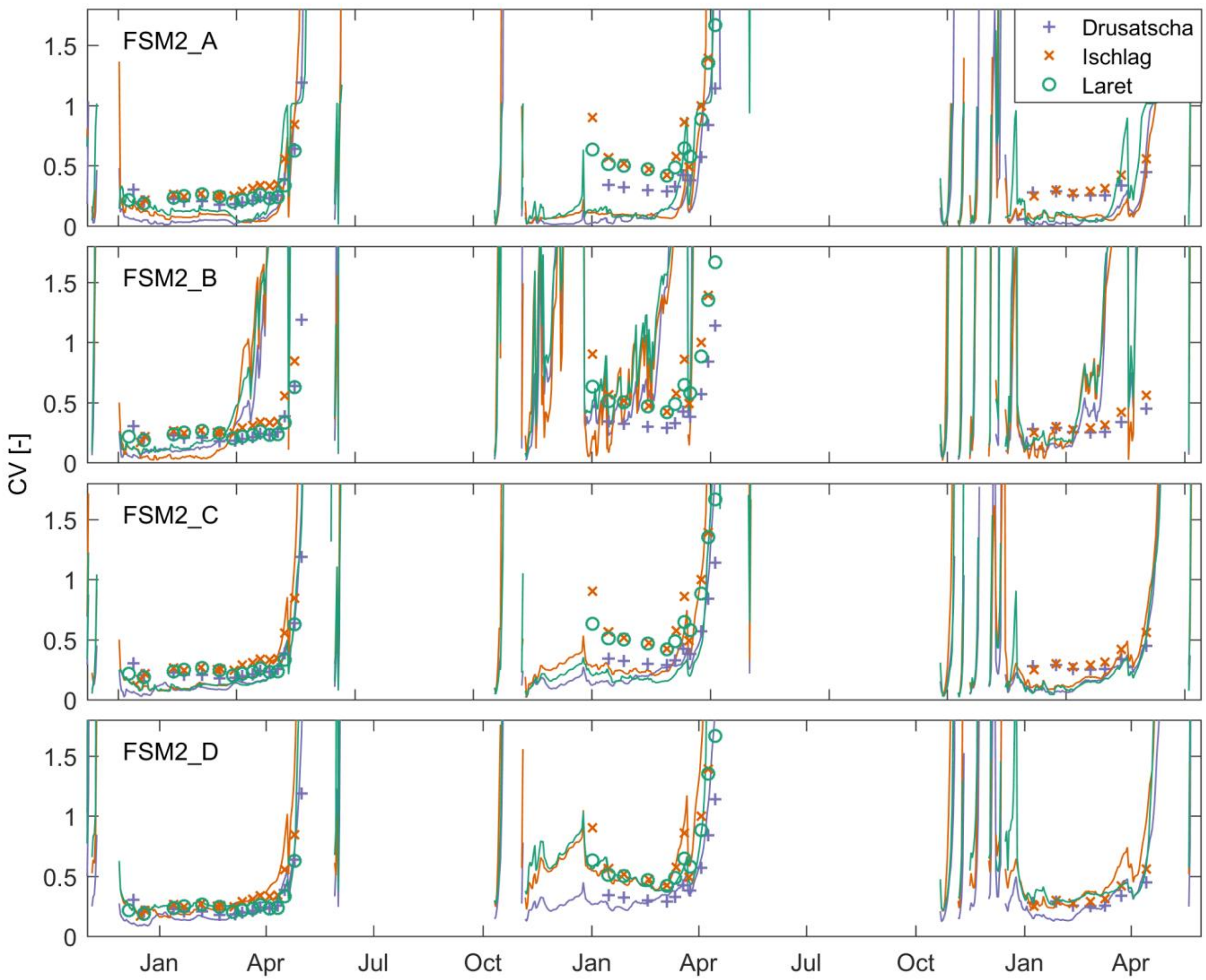

Figure 9: Temporal evolution of simulated (solid lines) and observed (symbols) coefficient of variation of snow depth (CV) at the three field areas for the four FSM2 versions.

4. Discussion

The spatial dynamics of snow accumulation and melt in forested environments is of great relevance for eco-hydrological processes (Lundquist & Dettinger 2005; Trujillo et al., 2012) and land-surface energy exchange (Liston, 2004; Loranty et al., 2014). They should hence be captured effectively in model applications from catchment to regional scales. Because mass and energy exchange processes are controlled by small-scale canopy-structural features, models require a high spatial resolution to explicitly resolve canopy-snow interactions (Clark et al., 2011a; Broxton et al., 2015). Recent efforts to incorporate such canopy-dependent process representations into forest snow models have generally increased model complexity at the expense of parsimony. Here, we have demonstrated that spatiotemporal forest snow distribution dynamics can also be reproduced with standard forest snow models commonly used in larger-scale applications. We have particularly showcased how the integration of local canopy information allowed accurate high-resolution (2m) simulations with only minor modifications to model structure.

Most modelling applications require spatial resolutions coarser than typical forest snow process scales (Blöschl, 1999; Clark et al. 2011a). Yet, they can benefit from high-resolution simulations in two ways: First, variability that arises from relevant but unresolved processes is commonly treated by sub-grid parametrizations, an example being the derivation of fractional snow-covered area from depletion curves (Essery & Pomeroy, 2004; Luce & Tarboton, 2004; Helbig et al., 2015). However, approaches specific to forested terrain are still rare (Czyzowska-Wisiniewski et al., 2015; Kostadinov et al., 2019) and further development of these methods demands data or simulations that depict realistic levels of spatial variability. While forest snow models set up based on stand-scale parameters (i.e. FSM2-A) underestimate spatial variations, simulations following the approach of FSM2-D are potentially suited to inform novel parameterizations of sub-grid variability. Second, model upscaling experiments can serve to investigate errors arising from model coarsening and corresponding spatial aggregation of canopy properties (e.g. Broxton et al., 2015). Respective studies may even lead to the derivation of effective canopy parameters suitable for coarser-scale simulations and/or correction functions to account for resolution-induced biases (Essery et al., 2009). To this end, single-model solutions that allow consistent process representation and coupling across spatial resolutions from meter to coarse grid scale constitute an ideal framework, rather than assuming transferability of results from a separate high resolution model to a coarse-scale model with a different set of parameterizations.

It is therefore a particular asset of our modelling approach that spatial accuracy is enhanced while the structure of standard, widely used models is preserved. More complex solutions put either high demands on computational resources and data availability, or do not easily translate to coarser scales if model structure changes are involved: For example, Musselman et al (2012b) introduced a space- and time-varying external input variable to account for direct-beam irradiance; the interception parametrization of Moeser et al. (2016) includes three dedicated canopy metrics and requires the model to track cumulative precipitation per storm event; and snowfall distribution as implemented by Broxton et al. (2015) relies on information about wind-direction dependent exposure at each modelled location. In FSM2-D however, spatial variability of energy balance terms is achieved by discerning near and distant canopy elements based on already used canopy descriptors, while preferential deposition and redistribution of snow are treated conceptually without necessitating horizontal coupling between grid cells.

FSM2-D achieves considerably improved performance with only minimal model changes, yet our approach also entails limitations. Disregarding directionality in radiation transfer may deteriorate model performance, particularly along forest edges during the ablation period where preferential melt is most evident (Mazzotti et al., 2019). Further, tree wells cannot be accurately resolved if very specific processes such as the bending of branches under snow load and subsequent unloading patterns are neglected (Sturm 1992). By confining canopy structure parameters to the widely used metrics LAI, V_F, CC_x and mCH_x, our modelling approach is essentially well suited to assess forest snow distribution over larger areas (Varhola et al. 2014). But the relevance of directional processes varies with climatic conditions and may hamper model transferability under certain circumstances, particularly (1) in dry high-isolation environments that feature pronounced discontinuities due to disturbances (Biederman et al., 2014; Harpold et al., 2014b), and (2) where forest snow is affected by wind-drift (Revuelto et al., 2015; Dickerson-Lange et al., 2017). Similar uncertainties arise when considering model transferability across different forest types. Like many other forest snow studies (Varhola et al., 2010), our work has been focused on evergreen conifer forests; but to date, datasets from deciduous stands are more scarce, and model applicability to these environments remains to be tested. In this context, the increasing availability of snow distribution datasets from airborne lidar offers more opportunities to further validate and improve the modeling approaches presented here.

Yet, the sole use of snow depth data for model performance assessment does not allow investigating potential equifinality issues and error compensation mechanisms (Beven, 2006; Clark et al., 2011b). Future forest snow model development and validation efforts should therefore also verify that the variability of individual processes is adequately captured. This is particularly important for processes that are controlled by local canopy-structure characteristics and thus exhibit strong spatial heterogeneity, such as shortwave radiation transfer, snow interception, and its subsequent unloading and sublimation. Experimental data that would have permitted process-level model evaluation were unfortunately not available at our sites for the period of this study. Follow-up research should leverage latest methods for the acquisition of spatially resolved micrometeorological data under heterogeneous canopy (Malle et al., 2019; Mazzotti et al. 2019b) to better constrain sub-canopy energy fluxes. Eventually, a multi-layer canopy representation may be needed to better resolve individual energy balance components that involve vertical gradients, for instance absorption of shortwave radiation and resulting canopy surface temperature inhomogeneities (Gouttevin et al., 2015; Webster et al., 2017).

5. Conclusion

This study has investigated how an energy-balance snow model of medium complexity coupled to a 1-layer canopy representation can be applied to realistically replicate small scale (<10m) variability of forest snow. Our results suggest that separate treatment of near and distant canopy elements allows balancing their impact on local energy exchange, mitigating discontinuity issues in canopy gaps and preventing overly rapid melt during ablation. Preferential deposition of precipitation and redistribution processes should be accounted for to create sufficient variability during snow accumulation. Both concepts were successfully implemented in FSM2 without increasing either model complexity or the number of canopy parameters involved, but with substantial improvements in model performance. The suggested approach is compatible with commonly used land surface models and may therefore allow a large community of model developers to assess their model in similar high-resolution applications.

Rapidly evolving remote sensing technologies and computational resources are increasing the availability of detailed canopy structure datasets and the potential to run high-resolution simulations over more and larger areas. In view of future work, we envision three cases: For regional scale applications, our single-model approach facilitates transference of process understanding gained from high-resolution simulations to coarser scales through intrinsic upscaling experiments. For catchment scale applications, the efficiency of the approaches presented here enables high resolution simulations that explicitly resolve canopy-snow interactions, even over entire watersheds. This provides unique opportunities to assess eco-hydrological implications of, e.g., natural and management–induced forest disturbances. For process-level studies, an approach that resolves detailed forest snow distribution patterns with commonly-used model concepts provides a suitable baseline for the evaluation of alternative, more complex process representations.

Acknowledgements

This project was funded by the Swiss National Science Foundation (SNF, projects 169213 and 200021_146184/1). Development of FSM2 is supported by NERC grant NE/P011926/1. C. D. Moeser was partially funded by the USGS South Central Climate Adaptation Science Center. We thank Pascal Egli, Saskia Gindraux, Nena Griessinger, Timea Marekova, Matthias Rieckh, Jiri Roubinek, Clare Webster, Franziska Zahner and Franziska Zieger from the SLF snow hydrology group for assistance in the field. We are particularly grateful to Clare Webster for providing synthethic hemispherical images and distributed sky view fraction calculations used to create the animations (SI), and for valuable input and discussions throughout the course of this work. We would further like to thank Adrian Harpold and Anne Nolin for their insightful and constructive reviews which helped improve the quality of this article. Data presented in this study are available from the WSL data repository Envidat (https://www.envidat.ch/dataset/forest-snow-modelling-davos-2012-2015). Any use of trade, firm, or product names is for descriptive purposes only and does not imply endorsement by the U.S. Government.

Appendix: Description of the FSM2 forest canopy model

The canopy energy balance in FSM2 largely follows Bewley et al. (2010). Shortwave transmission through the canopy is

$$\tau = \exp(-0.5\mathrm{VAI})$$

and the above-canopy albedo is

$$\alpha = (1 - \tau)\alpha_C + \tau^2\alpha_g$$

for dense canopy albedo α_c and ground albedo α_g, neglecting multiple reflections and assuming diffuse radiation. Snow cover fractions f_{cs} on the canopy and f_{gs} on the ground are used to interpolate between snow-free and snow-covered albedos (Essery, 2015). Net shortwave radiation absorbed by vegetation and the ground are

$$SW_v = (1 - \tau)(1 - \alpha_c + \alpha_g\tau)SW_\downarrow$$

and

$$SW_g = \left(1 - \alpha_g\right)\tau SW_\downarrow,$$

where $SW_\downarrow$ is the downwards shortwave radiation flux above the canopy. Assuming that vegetation and snow on the ground are blackbodies with surface temperatures T_v and T_g, net longwave radiation is

$$LW_v = (1 - \tau)(LW_\downarrow + \sigma T_g^4 - 2\sigma T_v^4)$$

and

$$LW_g = \tau LW_\downarrow - \sigma T_g^4 + (1 - \tau)\sigma T_v^4,$$

where σ is the Stefan-Boltzmann constant and $LW_\downarrow$ is the downwards longwave radiation flux above the canopy.

Momentum roughness lengths z_{0f} for snow-free ground and z_{0s} for snow are combined to give a ground roughness length

$$z_{0g} = z_{0f}^{1-f_s} z_{0s}^{f_s}.$$

For vegetation of height h covering fraction f_v of the ground, the roughness length and displacement height are $z_{0v} = 0.1h_c$ and $d = 0.67f_v h_c$. The combined roughness length is

$$z_0 = z_{0g}^{1-f_v} z_{0v}^{f_v}.$$

Neglecting the influences of atmospheric stability, aerodynamic resistances for heat transfer are

$$r_a = \frac{1}{ku_*}\ln\left(\frac{z-d}{z_0}\right)$$

between the canopy air space and the atmosphere,

$$r_g = \frac{1}{ku_*}\left[\frac{1-f_v}{\ln 10} + 0.004f_v\right]^{-1}$$

between the ground and the canopy air space, and

$$r_v = \frac{20}{\mathrm{VAI}u_*^{1/2}}$$

between the vegetation and the canopy air space, where k is the von Kármán constant, z is the meteorological measurement height and

$$u_* = kU_a\left[\ln\left(\frac{z-d}{z_0}\right)\right]^{-1}$$

is the friction velocity for above-canopy wind speed U_a.

Sensible heat fluxes are parametrized as

$$H = \frac{\rho c_p}{r_a}(T_c - T_a)$$

between the canopy air space at temperature T_c and above-canopy air at temperature T_a,

$$H_g = \frac{\rho c_p}{r_g}(T_g - T_c)$$

between the ground and the canopy air space, and

$$H_v = \frac{\rho c_p}{r_v}(T_v - T_c)$$

between the vegetation and the canopy air space. Similarly, moisture fluxes are parametrized as

$$E = \frac{\rho}{r_a}(Q_c - Q_a)$$

between the canopy air space with humidity Q_c and above-canopy air with humidity Q_a,

$$E_g = \frac{\rho}{r_{ag}}\left[Q_{\mathrm{sat}}(T_g) - Q_c\right]$$

between the ground and the canopy air space, and

$$E_v = \frac{\rho}{r_{av}}\left[Q_{\mathrm{sat}}(T_v) - Q_c\right]$$

between the vegetation and the canopy air space, where Q_{sat} is the temperature-dependent saturation humidity if the vegetation and the ground are snow-covered. If they are not, moisture fluxes are limited by water availability factors depending on soil moisture.

The energy and mass conservation equations

$$H = H_g + H_v,$$

$$E = E_g + E_v,$$
$$LW_g + SW_g = G + H + L_s E_g + L_f M$$

and

$$LW_v + SW_v = H_v + L_s E_s + C_{\text{can}} \frac{dT_v}{dt}$$

form a set of equations for the unknown Q_c, T_c, T_s, T_v, ground heat flux G and melt rate M; L_f and L_s are latent heats for melting and sublimation of snow, and C_{can} is the canopy heat capacity, assumed to be proportional to VAI. The equations are linearized and solved iteratively.

The model for interception of falling snow by the canopy is based on Hedstrom and Pomeroy (1998) as implemented by Essery et al. (2003). If the canopy holds a mass of S_v at the beginning of a timestep of length δt with snow falling at rate S_f, the increase in intercepted mass over the timestep is

$$\delta S_v = (S_{\max} - S_v)\left[1 - \exp\left(-\frac{f_v S_f \delta t}{S_{\max}}\right)\right]$$

where $S_{\max} = 4.4\text{VAI}$ is the maximum canopy snow holding capacity. Snow unloads from the canopy at rate $\tau_u^{-1} S_v$ with different values of the time constant τ_u for cold and melting snow.

References

Bartlett, P.A., MacKay, M.D., & Verseghy, D.L. (2006) Modified snow algorithms in the Canadian land surface scheme: Model runs and sensitivity analysis at three boreal forest stands. *Atmosphere-Ocean 44*(3), 207-222. https://doi.org/10.3137/ao.440301.

Beniston, M. (2003) Climatic change in mountain regions: a review of possible impacts. *Climatic Change 59*, 5-31. https://doi.org/10.1023/A:1024458411589.

Beven, K. (2006) A manifesto for the equifinality thesis. *Journal of Hydrology*, *320*, 18-36. https://doi.org/10.1016/j.jhydrol.2005.07.007.

Biederman, J.A., Brooks, P.D., Harpold, A.A., Gochis, D.J., Gutman, E., Reed, D.E., Pendall, E., & Ewers, B.E. (2014) Multiscale observations of snow accumulation and peak snowpack following widespread, insect-induced lodgepole pine mortality. *Ecohydrology*, *7*, 150-162. https://doi.org/10.1002/eco.1342.

Bewley, D., Essery, R., Pomeroy, J., & Ménard, C. (2010) Measurements and modelling of snowmelt and turbulent heat fluxes over shrub tundra. *Hydrology and Earth System Sciences 14*, 1331-1340. https://doi.org/10.5194/hess-14-1331-2010.

Blöschl, G. (1999) Scaling issues in snow hydrology. *Hydrological Processes 13*, 2149-2175. https://doi.org/10.1002/(SICI)1099-1085(199910)13:14/15<2149::AID-HYP847>3.0.CO;2-8

Boone, A., Samuelsson, P., Gollvik, S., Napoly, A., Jarlan, L., Brun, E., & Decharme, B. (2017) The interactions between soil–biosphere–atmosphere land surface model with a multi-energy balance (ISBA-MEB) option in SURFEXv8 – Part 1: Model description. *Geoscientific Model Development 10*(2), 843-872. https://doi.org/10.5194/gmd-10-1621-2017.

Broxton, P.D., Harpold, A.A., Biederman, J.A., Troch, P.A., Molotch, N.P., & Brooks, P.D. (2015) Quantifying the effects of vegetation structure on snow accumulation and ablation in mixed-conifer forests. *Ecohydrology 8*(6), 1073-1094. https://doi.org/10.1002/eco.1565.

Chen, J.M., Rich, P.M., Gover, S.T., Norman, J.M., & Plummer, S. (1997) Leaf area index of boreal forests: Theory, techniques and measurements. *Journal of Geophysical Research 102*(D24), 14. https://doi.org/10.1029/97JD01107.

Clark, M.P., Hendrikx, J., Slater, A.G., Kavetski, D., Anderson, B., Cullen, N.J., et al. (2011a) Representing spatial variability of snow water equivalent in hydrologic and land-surface models: A review. *Water Resources Research 47*(7). https://doi.org/10.1029/2011WR010745.

Clark, M.P., Kavetski, D. and Fenicia, F. (2011b) Pursuing the method of multiple working hypotheses for hydrological modelling. *Water Resources Research 47(9*), W09301. https://doi.org/10.1029/2010WR009827.

Clark, M.P., Nijssen, B., Lundquist, J.D., Kavetski, D., Rupp, D.E., Woods, R.A., et al. (2015) A unified approach for process-based hydrologic modeling: 1. Modeling concept. *Water Resources Research 51*(4), 2498-2514. https://doi.org/10.1002/2015WR017198.

Conway, J.P., Pomeroy, J.W., Helgason, W.D., & Kinar, N.J. (2018) Challenges in Modeling Turbulent Heat Fluxes to Snowpacks in Forest Clearings. *Journal of Hydrometeorology 19*(10), 1599-1616. https://doi.org/10.1175/JHM-D-18-0050.1.

Currier, W.R., & Lundquist, J.D. (2018) Snow Depth Variability at the Forest Edge in Multiple Climates in the Western United States. *Water Resources Research 54*, 18. https://doi.org/10.1029/2018WR022553.

Currier, W.R., Pflug, J., Mazzotti, G., Jonas, T., Deems, J.S., Bormann, K.J., et al. (2019) Comparing aerial lidar observations with terrestrial lidar and snow-probe transects from NASA's 2017 SnowEx campaign. *Water Resources Research.* https://doi.org/10.1029/2018WR024533.

Czyzowska-Wisiniewski, E. H., van Leeuwen, W.J.D., Hirschboeck, K. K., Marsh, S. E. & Wisiniewski, W. T. (2015) Fractional snow cover estimation in complex alpine-forested environments using an artificial neural network. *Remote Sensing of Environment, 156,* 403-417. https://doi.org/10.1016/j.rse.2014.09.026.

Dickerson-Lange, S.E., Lutz, J.A., Gersonde, R., Martin, K.A., Forsyth, J.E., & Lundquist, J.D. (2015) Observations of distributed snow depth and snow duration within diverse forest structures in a maritime mountain watershed. *Water Resources Research 51*(11), 9353-9366. https://doi.org/10.1002/2015WR017873.

Dickerson-Lange, S.E., Gersonde, R., Hubbart, J.A., Link, T.E., Nolin, A.W., Perry, G.H:, Roth, T. R., et al. (2017) Snow disappearance timing is dominated by forest effects on snow accumulation in warm winter climates of the Pacific Northwest, United States. *Hydrological Processes 31*, 1846-1862. https://doi.org/ 10.1002/hyp.11144.

Egli, L., Jonas, T., & Meister, R. (2009) Comparison of different automatic methods for estimating snow water equivalent. *Cold Regions Science and Technology 57*(2-3), 107-115. https://doi.org/10.1016/j.coldregions.2009.02.008.

Ellis, C.R., Pomeroy, J.W., Brown, T., & MacDonald, J. (2010) Simulation of snow accumulation and melt in needleleaf forest environments. *Hydrology and Earth System Sciences 14*(6), 925-940. https://doi.org/10.5194/hess-14-925-2010.

Ellis, C.R., Pomeroy, J.W., & Link, T.E. (2013) Modeling increases in snowmelt yield and desynchronization resulting from forest gap-thinning treatments in a northern mountain headwater basin. *Water Resources Research 49*(2), 936-949. https://doi.org/10.1002/wrcr.20089.

Essery, R. (2015) A factorial snowpack model (FSM 1.0). *Geoscientific Model Development 8*(12), 3867-3876. https://doi.org/10.5194/gmd-8-3867-2015.

Essery, R., Bunting, P., Rowlands, A., Rutter, N., Hardy, J., Melloh, R., et al. (2008a) Radiative Transfer Modeling of a Coniferous Canopy Characterized by Airborne Remote Sensing. *Journal of Hydrometeorology 9*(2), 228-241. https://doi.org/10.1175/2007JHM870.1.

Essery, R., Morin, S., Lejeune, Y., & Ménard, C.B. (2013) A comparison of 1701 snow models using observations from an alpine site. *Advances in Water Resources 55*, 131-148. https://doi.org/10.1016/j.advwatres.2012.07.013.

Essery, R., Pomeroy, J., Ellis, C., & Link, T. (2008b) Modelling longwave radiation to snow beneath forest canopies using hemispherical photography or linear regression. *Hydrological Processes 22*(15), 2788-2800. https://doi.org/10.1002/hyp.6930.

Essery, R., Pomeroy, J., Parviainen, J., & Storck, P. (2003) Sublimation of Snow from Coniferous Forests in a Climate Model. *Journal of Climate 16*), 1855-1864. https://doi.org/10.1175/1520-0442(2003)016<1855:SOSFCF>2.0.CO;2.

Essery, R., Rutter, N., Pomeroy, J., Baxter, R., Stahli, M., Gustafsson, D., et al. (2009) SNOWMIP2: An Evaluation of Forest Show Process Simulations. *Bulletin of the American Meteorological Society 90*(8), 1120-1135. http://dx.doi.org/10.1175/2009BAMS2629.1.

Essery, R., & Pomeroy, J. (2004) Implications of spatial distributions of snow mass and melt rate for snow-cover depletion: theoretical considerations. *Annals of Glaciology 38*, 261-265. https://doi.org/10.3189/172756404781815275

Ginzler, C., & Hobi, M. (2015) Countrywide Stereo-Image Matching for Updating Digital Surface Models in the Framework of the Swiss National Forest Inventory. *Remote Sensing 7*(4), 4343-4370. https://doi.org/10.3390/rs70404343.

Gouttevin, I., Lehning, M., Jonas, T., Gustafsson, D., & Mölder, M. (2015) A two-layer canopy model with thermal inertia for an improved snowpack energy balance below needleleaf forest (model SNOWPACK, version 3.2.1, revision 741). *Geoscientific Model Development 8*(8), 2379-2398. https://doi.org/10.5194/gmd-8-2379-2015.

Gupta, H.V., Kling, H., Yilmaz, K.K., & Martinez, G.F. (2009) Decomposition of the mean squared error and NSE performance criteria: Implications for improving hydrological modelling. *Journal of Hydrology 377*(1-2), 80-91. https://doi.org/10.1016/j.jhydrol.2009.08.003.

Hardy, J.P., Melloh, R., Koenig, G., Marks, D., Winstral, A., Pomeroy, J.W., & Link, T. (2004) Solar radiation transmission through conifer canopies. *Agricultural and Forest Meteorology 126*(3-4), 257-270. https://doi.org/10.1016/j.agrformet.2004.06.012.

Harpold, A.A., Guo, Q., Molotch, N., Brooks, P.D., Bales, R., Fernandez-Diaz, J.C., et al. (2014) LiDAR-derived snowpack data sets from mixed conifer forests across the Western United States. *Water Resources Research 50*(3), 2749-2755. https://doi.org/10.1002/2013WR013935.

Harpold, A.A., Biederman, J.A., Condon, K:, Merino, M., Korgaonkar, Y:, Nan, T., Sloat, L.L., et al. (2014b) Changes in snow accumulation and ablation following the Las Conchas Forest Fire, New Mexico, USA. *Ecohydrology, 7*, 440-452. https://doi.org/10.1002/eco.1363.

Hedstrom, N., & Pomeroy, J.W. (1998) Measurements and modelling of snow interception in the boreal forest. *Hydrological Processes 12*, 1611-1625. https://doi.org/10.1002/(SICI)1099-1085(199808/09)12:10/11<1611::AID-HYP684>3.0.CO;2-4.

Helbig, N., van Herwijnen, A., Magnusson, J., & Jonas, T. (2015) Fractional snow-covered area parameterization over complex topography. *Hydrology and Earth System Sciences 19*(3), 1339-1351. https://doi.org/10.5194/hess-19-1339-2015.

Hiemstra, C.A., Liston, G.E., & Reiners, W.A. (2006) Observing, modelling, and validating snow redistribution by wind in a Wyoming upper treeline landscape. *Ecological Modelling 197*(1-2), 35-51. https://doi.org/10.1016/j.ecolmodel.2006.03.005

Khosravipour, A., Skidmore, A.K., Isenburg, M., Wang, T., & Hussin, Y.A. (2014) Generating Pit-free Canopy Height Models from Airborne Lidar. *Photogrammetric Engineering & Remote Sensing 80*(9), 863-872. https://doi.org/10.14358/PERS.80.9.863.

Lawler, R.R., & Link, T.E. (2011) Quantification of incoming all-wave radiation in discontinuous forest canopies with application to snowmelt prediction. *Hydrological Processes 25*(21), 3322-3331. https://doi.org/10.1002/hyp.8150.

Lehning, M., Löwe, H., Ryser, M., & Raderschall, N. (2008) Inhomogeneous precipitation distribution and snow transport in steep terrain. *Water Resources Research 44*(7). https://doi.org/10.1029/2007WR00654.

Lehning, M., Völksch, I., Gustafsson, D., Nguyen, T.A., Stähli, M., & Zappa, M. (2006) ALPINE3D: a detailed model of mountain surface processes and its application to snow hydrology. *Hydrological Processes 20*(10), 2111-2128. https://doi.org/10.1002/hyp.6204.

Liston, G.E. (2004) Representing Subgrid Snow Cover Heterogeneities in Regional and Global Models. *Journal of Climate 17*(1381-1397). https://doi.org/10.1175/1520-0442(2004)017<1381:RSSCHI>2.0.CO;2.

Luce, C.H., & Tarboton, D.G. (2004) The application of depletion curves for parameterization of subgrid variability of snow. *Hydrological Processes 18*(8), 1409-1422. https://doi.org/10.1002/hyp.1420.

Lundquist, J.D., & Dettinger, M.D. (2005) How snowpack heterogeneity affects diurnal streamflow timing. *Water Resources Research 41*(5). https://doi.org/10.1029/2004WR003649.

Lundquist, J.D., Dickerson-Lange, S.E., Lutz, J.A., & Cristea, N.C. (2013) Lower forest density enhances snow retention in regions with warmer winters: A global framework developed from plot-scale observations and modeling. *Water Resources Research 49*(10), 6356-6370. https://doi.org/100.1002/wrcr.20504.

MacKay, M.D., & Bartlett, P.A. (2006) Estimating canopy snow unloading timescales from daily observations of albedo and precipitation. *Geophysical Research Letters 33*(19). https://doi.org/10.1029/2006GL027521.

Magnusson, J., Eisner, S., Huang, S., Lussana, C., Mazzotti, G., Essery, R., et al. (2019) Influence of spatial resolution on snow cover dynamics for a coastal and mountainous region at high latitudes (Norway). *Water Resources Research 55*. https://doi.org/10.1029/2019WR024925.

Magnusson, J., Gustafsson, D., Hüsler, F., & Jonas, T. (2014) Assimilation of point SWE data into a distributed snow cover model comparing two contrasting methods. *Water Resources Research 50*(10), 7816-7835. https://doi.org/10.1002/2014WR015302.

Magnusson, J., Wever, N., Essery, R., Helbig, N., Winstral, A., & Jonas, T. (2015) Evaluating snow models with varying process representations for hydrological applications. *Water Resources Research 51*(4), 2707-2723. https://doi.org/10.1002/2014WR016498.

Mahat, V., & Tarboton, D.G. (2012) Canopy radiation transmission for an energy balance snowmelt model. *Water Resources Research 48*(1). https://doi.org/10.1029/2011WR010438.

Mahat, V., & Tarboton, D.G. (2014) Representation of canopy snow interception, unloading and melt in a parsimonious snowmelt model. *Hydrological Processes 28*(26), 6320-6336. https://doi.org/10.1002/hyp.10116.

Mahat, V., Tarboton, D.G., & Molotch, N.P. (2013) Testing above- and below-canopy representations of turbulent fluxes in an energy balance snowmelt model. *Water Resources Research 49*(2), 1107-1122. https://doi.org/10.1002/wrcr.20073.

Malle, J., Rutter, N., Mazzotti, G., & Jonas, T. (2019) Shading by Trees and Fractional Snow Cover Control the Subcanopy Radiation Budget. *Journal of Geophysical Research: Atmospheres 124*(6), 3195-3207. https://doi.org/10.1029/2018JD029908.

Marty, C., Tilg, A.-M., & Jonas, T. (2017) Recent Evidence of Large-Scale Receding Snow Water Equivalents in the European Alps. *Journal of Hydrometeorology 18*(4), 1021-1031. https://doi.org/10.1175/JHM-D-16-0188.1.

Mazzotti, G., Currier, W.R., Deems, J.S., Pflug, J.M., Lundquist, J.D., & Jonas, T. (2019a) Revisiting Snow Cover Variability and Canopy Structure Within Forest Stands: Insights From Airborne Lidar Data. *Water Resources Research*. https://doi.org/10.1029/2019WR024898.

Mazzotti, G., Malle, J., Barr, S., & Jonas, T. (2019b) Spatially continuous characterization of forest canopy structure and sub-canopy irradiance derived from handheld radiometer surveys. *Journal of Hydrometeorology 20*(7), 1417 – 1433. https://doi.org/10.1175/JHM-D-18-0158.1.

Melloh, R.A., Hardy, J. P., Bailey, R. N. & Hall, T.J. (2002). An efficient snow albedo model for the open and the sub-canopy. *Hydrological Processes 16*, 3571-3584. https://doi.org/10.1002/hyp.1229.

Miller, J.B. (1967) A formula for average foliage density. *Australian Journal of Botany 15*(1), 4.

Moeser, D., Mazzotti, G., Helbig, N., & Jonas, T. (2016) Representing spatial variability of forest snow: Implementation of a new interception model. *Water Resources Research 52*, 1208-1226. https://doi.org/10.1002/2014WR016724.

Moeser, D., Morsdorf, F., & Jonas, T. (2015a) Novel forest structure metrics from airborne LiDAR data for improved snow interception estimation. *Agricultural and Forest Meteorology 208*, 40-49. https://doi.org/10.1016/j.agrformet.2015.04.013.

Moeser, D., Roubinek, J., Schleppi, P., Morsdorf, F., & Jonas, T. (2014) Canopy closure, LAI and radiation transfer from airborne LiDAR synthetic images. *Agricultural and Forest Meteorology 197*, 158-168. https://doi.org/10.1016/j.agrformet.2014.06.008.

Moeser, D., Stähli, M., & Jonas, T. (2015b) Improved snow interception modeling using canopy parameters derived from airborne LiDAR data. *Water Resources Research 51*(7), 5041-5059. https://doi.org/10.1002/2014WR016724.

Murray, C.D., & Buttle, J.M. (2003) Impacts of clearcut harvesting on snow accumulation and melt in a northern hardwood forest. *Journal of Hydrology 271*(197-212). https://doi.org/10.1016/S0022-1694(02)000352-9.

Musselman, K.N., Molotch, N.P., Margulis, S.A., Kirchner, P.B., & Bales, R.C. (2012a) Influence of canopy structure and direct beam solar irradiance on snowmelt rates in a mixed conifer forest. *Agricultural and Forest Meteorology 161*, 46-56. https://doi.org/10.1016/j.agrformet.2012.03.011.

Musselman, K.N., Molotch, N.P., Margulis, S.A., Lehning, M. & Gustafsson, D. (2012b) Improved snowmelt simulations with a canopy model forced with photo-derived direct beam canopy transmissivity. *Water Resources Research 48*(10). https://doi.org/10.1029/2012WR012285.

Musselman, K. N., Pomeroy, J. W., & Link, T. E. (2015). Variability in shortwave irradiance caused by forest gaps: Measurement, modelling, and implications for snow energetics.

Agricultural and Forest Meteorology 207, 62-82. https://doi.org/10.1016/j.agrformet.2015.03.014.

Oleson, K.W., Lawrence, D.M., Bonan, G.B., Drewniak, B., Huang, M., Koven, C.D., et al. (2013) Technical description of version 4.5 of the Community Land Model (CLM). NCAR Technical Note. https://doi.org/10.5065/D6RR1W7M.

Pomeroy, J., Parviainen, J., Hedstrom, N., & Gray, D. (1998) Coupled modelling of forest snow interception and sublimation. *Hydrological Processes 12*(15), 2317-2337. https://doi.org/10.1002/(SICI)1099-1085(199812)12:15<2317::AID-HYP799>3.0.CO;2-X.

Pomeroy, J.W., Marks, D., Link, T., Ellis, C., Hardy, J., Rowlands, A., & Granger, R. (2009) The impact of coniferous forest temperature on incoming longwave radiation to melting snow. *Hydrological Processes 23*(17), 2513-2525. https://doi.org/10.1002/hyp.7325.

Revuelto, J., Lopez-Moreno, J.I:, Azorin-Molina, C., & Vicente-Serrano, S.M. (2015) Canopy influence on snow depth distribution in a pine stand determined from terrestrial laser data. *Water Resources Research, 51,* 3476-3489. https://doi.org/10.1002/2014WR016496.

Roth, T.R., & Nolin, A.W. (2017) Forest impacts on snow accumulation and ablation across an elevation gradient in a temperate montane environment. *Hydrology and Earth System Sciences 21*(11), 5427-5442. https://doi.org/10.5194/hess-21-5427-2017.

Roth, T.R., & Nolin, A.W. (2019) Characterizing Maritime Snow Canopy Interception in Forested Mountains. *Water Resources Research 55*(6), 4564-4581. https://doi.org/10.1029/2018WR024089.

Rutter, N., Essery, R., Pomeroy, J., Altimir, N., Andreadis, K., Baker, I., et al. (2009) Evaluation of forest snow processes models (SnowMIP2). *Journal of Geophysical Research 114*(D6). https://doi.org/10.1029/2008JD011063.

Schleppi, P., Conedera, M., Sedivy, I., & Thimonier, A. (2007) Correcting non-linearity and slope effects in the estimation of the leaf area index of forests from hemispherical photographs. *Agricultural and Forest Meteorology 144*(3-4), 236-242. https://doi.org/10.1016/j.agrformet.2007.02.004.

Schneider, E.E., Affleck, D.L.R., & Larson, A.J. (2019) Tree spatial patterns modulate peak snow accumulation and snow disappearance. *Forest Ecology and Management 441*, 9-19. https://doi.org/10.1016/j.foreco.2019.03.031.

Sohrabi, M.M., Tonina, D., Benjankar, R., Kumar, M., Kormos, P., Marks, D., & Luce, C. (2019) On the role of spatial resolution on snow estimates using a process-based snow model across a range of climatology and elevation. *Hydrological Processes 33*(8), 1260-1275. https://doi.org/10.1002/hyp.13397.

Sturm, M. (1992) Snow distribution and heat flow in the taiga. *Arctic and Alpine Research 24(2)*, 145-152. https://doi.org/10.1080/00040851.1992.12002939.

Sun, N., Wigmosta, M., Zhou, T., Lundquist, J., Dickerson-Lange, S., & Cristea, N. (2018) Evaluating the functionality and streamflow impacts of explicitly modelling forest-snow interactions and canopy gaps in a distributed hydrologic model. *Hydrological Processes 32*(13), 2128-2140. https://doi.org/10.1002/hyp.13150.

Tape, K.E.N., Sturm, M., & Racine, C. (2006) The evidence for shrub expansion in Northern Alaska and the Pan-Arctic. *Global Change Biology 12*(4), 686-702. https://doi.org/10.1111/j.1365-2486.2006.01128.x.

Trujillo, E., Molotch, N.P., Goulden, M.L., Kelly, A.E., & Bales, R.C. (2012) Elevation-dependent influence of snow accumulation on forest greening. *Nature Geoscience 5*(10), 705-709. https://doi.org/10.1038/NGEO1571.

Varhola, A., & Coops, N.C. (2013) Estimation of watershed-level distributed forest structure metrics relevant to hydrologic modeling using LiDAR and Landsat. *Journal of Hydrology 487*, 70-86. https://doi.org/10.1016/j.jhydrol.2013.02.032.

Varhola, A., Coops, N.C., Weiler, M., & Dan Moore, R. (2010) Forest canopy effects on snow accumulation and ablation: An integrative review of empirical results. *Journal of Hydrology 392*, 219-233. https://doi.org/10.1016/j.jhydrol.2010.08.009.

Varhola, A., Coops, N.C., Alila, Y., & Weiler, M. (2014) Exploration of remotely sensed forest structure and ultrasonic range sensor metrics to improve empirical snow models. *Hydrological Processes 28*(15), 4433-4448. https://doi.org/10.1002/hyp.9952.

Vionnet, V., Brun, E., Morin, S., Boone, A., Faroux, S., Le Moigne, P., et al. (2012) The detailed snowpack scheme Crocus and its implementation in SURFEX v7.2. *Geoscientific Model Development 5*(3), 773-791. https://doi.org/10.5194/gmd-5-773-2012.

Vögeli, C., Lehning, M., Wever, N., & Bavay, M. (2016) Scaling Precipitation Input to Spatially Distributed Hydrological Models by Measured Snow Distribution. *Frontiers in Earth Science* 4. https://doi.org/10.3389/feart.2016.00108.

Webster, C., Rutter, N., Zahner, F. & Jonas, T. (2016) Modeling subcanopy incoming longwave radiation to seasonal snow using air and tree trunk temperatures. *Journal of Geophysical Research: Atmospheres 121*(3), 1220-1235. https://doi.org/10.1002/2015JD024099.

Webster, C., Rutter, N., & Jonas, T. (2017) Improving representation of canopy temperatures for modeling subcanopy incoming longwave radiation to the snow surface. *Journal of Geophysical Research: Atmospheres 122*, 9154-9172. https://doi.org/10.1002/2017JD026581.

Wever, N., Fierz, C., Mitterer, C., Hirashima, H., & Lehning, M. (2014) Solving Richards Equation for snow improves snowpack meltwater runoff estimations in detailed multi-layer snowpack model. *The Cryosphere 8*(1), 257-274. https://doi.org/10.5194/tc-8-257-2014.

Winstral, A., Elder, K., & Davis, R.E. (2002) Spatial Snow Modeling of Wind-Redistributed Snow Using Terrain-Based Parameters. *Journal of Hydrometeorology 3*, 524-538. https://doi.org/10.1175/1525-7541(2002)003<0524:SSMOWR>2.0.CO;2